THE JOURNAL OF PHYSICAL CHEMISTRY A

Article

pubs.acs.org/JPCA

Taming the Electronic Structure of Diradicals through the Window of Computationally Cost Effective Multireference Perturbation Theory

Suvonil Sinha Ray, Anirban Ghosh, and Sudip Chattopadhyay*

Department of Chemistry, Indian Institute of Engineering Science and Technology, Shibpur, Howrah 711103, India

Rajat K. Chaudhuri

Theoretical Physics, Indian Institute of Astrophysics, Bangalore 560034, India

ABSTRACT: Recently a state-specific multireference perturbation theory (SSMRPT) with an improved virtual orbitals complete active space configuration interaction (IVO-CASCI) reference function has been proposed for treating electronic structures of radicals such as methylene, *m*-benzyne, pyridyne, and pyridynium cation. This new development in MRPT, termed as IVO-SSMRPT, ensures that it is able to describe the structure of radicaloids with reasonable accuracy even with small reference spaces. IVO-SSMRPT is also capable of predicting the correct ordering of the lowest singlet−triplet gaps. Investigation of the first three electronic states of the oxygen molecule has also been used for rating our method. The agreement of our estimates with the available far more expensive benchmark *state-of-the-art ab initio* calculations is creditable. The IVO-SSMRPT method provides an effective avenue with manageable cost/accuracy ratio for accurately dealing with radicaloid systems possessing varying degrees of quasidegeneracy.

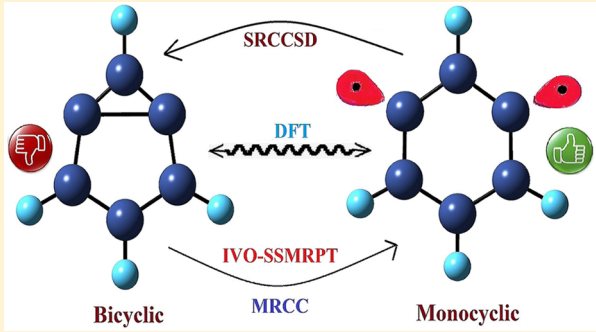

I. INTRODUCTION

The diradicals delineate an important class of compounds due to the presence of weakly interacting unpaired electrons (furnish near degenerate low-lying electronic states of different spin) and have been the subject of many experimental as well as theoretical investigations due to their high reactivity and significance as common intermediates or transition states for many organic and inorganic chemical processes.[1] As per Salem,[2] diradicals can be viewed as molecular systems with two electrons occupying two quasi-degenerate orbitals. Diradicals play a pivotal role in various biological processes, say, isomerization of the retinal chromophore associated with the mechanism of vision. Investigations of radicaloids are also useful to understand the weak interatomic and intermolecular interactions in large systems. The development of accurate as well as computationally cost-effective methods for the reliable description of quasidegenerate nature of radicals poses a challenging problem for contemporary quantum-computational chemistry.[3,4] It is generally very difficult to get reliable information about radical intermediates by experimental techniques due to their short lifetimes.

A correct treatment of both the nondynamic (accounts for nearly degenerate electron configurations) and the dynamical correlation (brought out by the interaction of the virtual functions obtained by excitation of electrons from the mean field function) is a necessary prerequisite to characterize the electronic structure of diradicals. These two correlation effects are coupled, and modeling these two contributions in a balanced manner is one of the major challenges of modern electronic structure theory. The conventional single reference-(SR) methods are inadequate in treating the quasidegeneracy in diradicals. Note that when electron configurations become exactly or very nearly degenerate (e.g., for radicaloids), a multireference(MR) treatment may be necessary. To get a correct quantitative (and sometimes even qualitative) description, an appropriate MR zero-order wave function should be augmented by the effect of dynamical correlation. A number of approaches that can incorporate dynamic correlation have been established, including multireference perturbation theory (MRPT),[5−9] MR configuration interaction (MRCI),[10] or multireference coupled-cluster (MRCC) corrections.[11] Among these methods, the MRCI (does not provide size-extensive energies when truncated) and MRPT are the most commonly used theoretical methods, while MRCC methods have not yet been established as practical tools for routine use, although they are expected to provide more accurate results than the MRCI or MRPT methods. The concrete logical framework of the working principle, the ease of numerical implementation and the underlying capability of possible hierarchical improvement in the formulation of the basic theoretical constructs make the

Received: March 30, 2016
Revised: June 29, 2016
Published: June 29, 2016

DOI: 10.1021/acs.jpca.6b03211
J. Phys. Chem. A 2016, 120, 5897−5916

MRPT a widely used efficient approach for treating dynamical electron correlation.

It should be noted that the development of size-extensive PT (and also CC) methods, based on the MR/MC description of the reference function, are neither unique nor straightforward. There are different theories of varying degrees of sophistication and they emphasize different aspects of correlation and ease of computation. Thus, the formulation and implementation of MRPT formalisms is a burgeoning frontier area of research in electronic structure theory. Historically, the oldest approaches to the MRPT worked within the framework of effective Hamiltonians where one simultaneously targeted all eigenvalues of the effective Hamiltonian. Conventional effective Hamiltonian based formalisms suffer from convergence problem due to the intruder states causing appearance of very small energy denominators in PT series and require computation of states one is not interested in. The intruder states being energetically proximate with the model space function with respect to the zeroth-order Hamiltonian and not in regard to the true Hamiltonian, are attributed as perturber states. Many of the MR perturbation theories are fraught with the problem, at the zeroth order, that states appear to be almost degenarate when no such degeneracy appears in reality. To overcome this problem, one can relax the restrictions of multiroot eigenvalues on the effective Hamiltonian approaches and demand instead that the effective Hamiltonian operator diagonalized in the active space provides fewer roots which are physically meaningful and eigenvalues of the Hamiltonian while the rest are spurious. This is the so-called Intermediate Hamiltonian formalism which has been suggested by Kirtman[12] and developed much more efficiently by Malrieu et al.[13] An extreme example of the intermediate Hamiltonian method is the single-root/state-specific approach where one constructs the effective Hamiltonian in the active space but targets only one root of physical interest.

The popular *state-of-the-art* MRPT approaches which have the ability to compute the state energy in a target (state) specific manner are the complete active space (CAS) second-order perturbation (CASPT2),[14,15] second-order multireference Møller−Plesset (MRMP2),[16,17] and *n*-electron valence state perturbation theory at second order (NEVPT2).[18,19] These methods are not rigorously size-extensive in nature.[20,21] Although single-root in nature, both CASPT2 and MRMP2 methods are not manifestly intruder free[22,23] and can be remedied by using the level shift technique.[22−24] It has been argued that NEVPT2 is inherently less prone to the intruder problem as compared with MRMP2 and CASPT2.[25] The inflexibility of the CASPT2, MRMP2, and NEVPT2 methods can be ameliorated by the formulation of their multistate version,[26−29] in which the wave functions of different states are allowed to mix in the presence of dynamical correlation. There are the extension of the MCQDPT and MS-CASPT2 methods with greater flexibility which are known as X-MCQDPT2 (due to Granovsky)[30] and XMS-CASPT2 (as developed by Shiozaki et al. based on Granovsky's work).[31] All these MS-approaches are more or less directly related to the formal theory of the effective Hamiltonians of QDPT that have been well established for a long time. Hence, they can be plagued by the intruder state problem and the level shift technique or similar techniques can be exploited to avoid these problems.[22−24]

The CAS based state-specific MRPT method (SSMRPT) of Mukherjee and co-workers[32] [*aka* MkMRPT in the literature due to Evangelista et al.[33]] has established itself as an efficient method for treating quasidegeneracy in the presence of intruder effect without adding any *ad hoc* level-shift. Unlike the widely used CAS-based MRPTs mentioned above, the SSMRPT method of Mukherjee and co-workers[32] is intrinsically flexible in the sense that it can be used in a manner that it can relax the coefficients of the reference wave function (as a result of coupling of the nondynamical and dynamical correlations via the diagonalization of the dressed or effective Hamiltonian), or keep the coefficients frozen if required. Other redeeming features of the SSMRPT method[32] are (i) it can be cast in various forms using Møller−Plesset and Epstein−Nesbet multipartitioning strategy within the framework of Rayleigh−Schrödinger (RS) and Brillouin-Wigner perturbative expansions,[32] (ii) it is manifestly size extensive, (iii) it is size-consistent (with localized orbitals), and (iv) it is computationally affordable. Thus, the SSMRPT method encompasses almost all the desirable properties that a MR method should have, and thus it seems worthwhile to investigate its performance for numerous systems as is evident from the published works.[32,34−38] The method has also been employed for studying dissociation surfaces for electronic states of molecules containing medium heavy atoms.[39]

In the CAS-based SSMRPT calculations, the reference functions have usually been generated via CAS self-consistent field (CASSCF) calculations. The highly nonlinear nature of the working equations of CASSCF method may lead (i) to convergence difficulties and (ii) multiple solutions corresponding to minima (thus making it difficult to find the orbitals corresponding to the global minimum).[40] To ameliorate these objections, few effective alternatives have also been proposed and implemented.[41−47] Improved virtual orbitals (IVO) CAS configuration interaction (IVO-CASCI) is an effective alternative method, which does not involve iterations beyond those in the initial SCF calculation altogether. It does not possess features that create convergence difficulties with increasing size of the CAS in CASCI calculations. The elimination of the nonlinear simultaneous optimization of orbital and CI coefficients can lead not only to a reduction in computational cost but also to an improved qualitative description of the energy surface. The IVO-CASCI method has been quite effective to describe not only the near equilibrium region (where the RHF equations are usually readily solved) but also the bond-breaking region (where convergence of the RHF equations is challenging) of the energy surfaces.[41−47] In nutshell, it provides a balanced treatment of the most important electron configurations that contribute to a correlated wave function.

Prompted by the success of MRMP2 and MCQDPT schemes using IVO-CASCI function,[48−50] very recently, we have suggested an SSMRPT method using IVO-CASCI reference functions (IVO-SSMRPT), rather than the CASSCF functions, and demonstrated that IVO-SSMRPT is comparable in accuracy to CASSCF-SSMRPT.[51] It has been primarily used for handling of ground states, although, in principle, it is designed to access any state, ground or excited. In the present paper, we employ IVO-SSMRPT to calculate geometrical parameters in methylene (CH_2), benzyne (C_6H_4), pyridyne (C_5NH_3), and pyridynium cation ($C_5NH_4^+$). The dissociation energy surface/curve of O_2 in its ground (triplet) and lowest two singlet excited electronic states have also been investigated by our IVO-SSMRPT method. An appropriate description of the (single/or multiple) bond dissociation process is still a

DOI: 10.1021/acs.jpca.6b03211
J. Phys. Chem. A 2016, 120, 5897−5916

challenge for the contemporary theoretical chemist since a proper and balanced treatment of two types of electron correlation, nondynamic and dynamic, is required when we have to deal with bond dissociation process. Our results have been compared with *state-of-the-art* results and experimental data, if available. The IVO-CASCI function has already been used in the past to study radicaloids.[52,53] It should be noted that the prime aim of the work is not to answer the still open questions of interpretation of electronic structure of the systems investigated but rather to judge the efficacy of the newly developed IVO-SSMRPT to provide a viable means of calculation of singlet and nonsinglet states of radicals. The electronic structures of diradicals have been extensively studied by Krylov and co-workers, using either the spin-flip (SF) approach[54,55] as well as the more general equation-of-motion (EOM) CC method of both SF-type (EOM-SF-CCSD) and EOM-CC(2,3)-type.[56]

There are also other very interesting MRPT formulations like Brillouin−Wigner perturbation theory,[57,58] multiconfiguration PT (MCPT),[59] antisymmetrized product of strongly orthogonal geminals based PT (APSG-PT),[60,61] block-correlated PT,[62] the so-called static-dynamic-static (SDS) PT,[63] the restricted active space perturbation theory, RASPT2,[64] quasicomplete active space quasi-degenerate perturbation theory (QCASQDPT),[65] general MCQDPT (GMCQDPT),[66] the reduced model space MRMP2[67] and so on. In this context, we should mention that the quasi-degenerate perturbation theory based on the occupation restricted multiple active space (ORMAS-PT) is an efficient approximation to the MRMP2/MCQDPT level of theory. Akin to the restricted active space self-consistent field (RASSCF) and quasi-complete active space (QCAS), the ORMAS expands the wave function within a basis that is typically much smaller than the corresponding CAS basis. In order to avoid higher-order reduced density matrices (and also to simplify the analytical energy gradients), the partially contracted scheme has also been proposed by Werner and co-workers for CASPT2.[31,68,69] Another interesting development is the generalized van Vleck PT (GVVPT) of Hoffmann and co-workers.[70,71] They showed the way to tackle large active spaces via the use of macroconfigurations and also discusses very nicely how to avoid the intruder problem.

To conclude the Introduction, we should mention the developments based on DMRG (density matrix renormalization group) with the target of studying medium-to-large molecular systems by MR computations.[43] Moreover, in recent time, a new integrated, cost-effective and robust strategy for accurate MR variational/perturbative calculations for large-size systems (e.g., open shell organic radicaloids) where the static correlation plays an important role has been suggested and validated through the development of BALOO package by the group of Cacelli and co-workers.[72−75]

The rest of the paper is organized as follows. Section II provides a brief resumé of basic ingredients of SSMRPT method after recalling the main features of the IVO-CASCI approach. In section III, we address the application of gradient technique of IVO-CASCI-based SSMRPT approach to a few significant test cases such as computation of (i) optimized geometrical parameters of methylene, *m*-benzyne, pyridyne, and pyridynium cation molecules, and (ii) singlet−triplet gaps for methylene, and *m*-benzyne. The singlet−triplet gap has been computed as a difference of the two separate individual energy calculations for the singlet and triplet states. The equilibrium geometries of the singlet and triplet states of diradicals may be somewhat different, which may have an influence on their magnetic properties. Section(IV contains summarizing remarks pertaining to our the present work. We envisage that the IVO-SSMRPT serves the purpose of a good theoretical strategy to tackle strongly quasi-degenrate situations via an appropriate treatment of the dynamical and nondynamical correlation effects in a cost-effective fashion and has all the potentiality to deal with a host of ground and excited electronic states, where many other standard electronic structure methods tend to be unusable.

II. ESSENTIAL INGREDIENTS OF THE IVO-SSMRPT THEORY

II.A. SSMRPT: A Brief Resumé. In this section we will provide a brief resume of those aspects of the SSMRPT and IVO-CASCI method, which are relevant to our arriving at the IVO-SSMRPT approach.

In SSMRPT, the initial target function expanded in terms of the multiexponential Jeziorski−Monkhorst (JM) ansatz[76]

$$|\psi\rangle = \sum_{\mu} \exp(T_\mu)|\phi_\mu\rangle c_\mu \tag{1}$$

involves a separate cluster-operator T_μ, obtained for each model-space function. Here, ϕ_μ is a model function in a CAS. None of T_μ operators can produce excitations within the model space (intermediate normalization). This multiexponential Ansatz is very effective when we have to deal with the interplay of two types of electron correlation: nondynamic and dynamic. Note that JM ansatz-based methods are much better suited for studies of molecular energy surfaces rather than the energy difference of spectroscopic interest.

Equations determining the cluster amplitudes have been derived by inserting the JM ansatz into the Schrödinger equation, assuming a set of redundancy conditions characteristic for the state specific parametrization of the JM ansatz. Equations providing the cluster amplitudes at the first order take the following form in the frame of Rayleigh−Schrödinger (RS) perturbation theory (RSPT) with Møller−Plesset (MP) multipartitioning of the Hamiltonian

$$t_\mu^{l(1)}(\mu) = \frac{H_{l\mu} + \sum_\nu^{\nu\neq\mu} t_\mu^{l(1)}(\nu) H_{\mu\nu}(c_\nu^0/c_\mu^0)}{(E_{\mathrm{CAS}} - H_{\mu\mu}) + (E_{0,\mu\mu} - E_{0,ll})} \tag{2}$$

with $\langle\chi_l^\mu|T_\mu^{l(1)}|\phi_\mu\rangle = t_\mu^{l(1)}(\mu)$,$\langle\chi_l^\mu|T_\nu^{l(1)}|\phi_\mu\rangle = t_\mu^{l(1)}(\nu)$, $\langle\phi_\mu|H|\phi_\nu\rangle = H_{\mu\nu}$, and $\langle\chi_l^\mu|H|\phi_\mu\rangle = H_{l\mu}$. Here, $\{\chi_l^\mu\}$ is a virtual function emerging from a model function by the action of T_μ on ϕ_μ. In the above equation, E_{CAS} stands for the CAS (rather CASCI of the reference state) energy corresponding to frozen coefficients c_μ^0 for the reference functions obtained from diagonalization of $\sum_\nu H_{\mu\nu}\, c_\nu^0 = E_{\mathrm{CAS}}\, c_\mu^0$. Here, E_0 is the expectation value of H_0 with respect to a specific configuration. H_0 has a "general diagonal" form such that, for a CAS, the model and the virtual functions are in no way connected by H_0. However, such a structure in no way necessitates that H_0 be strictly diagonal, instead, it is sufficient that H_0 accounts for the scattering among the doubly occupied core orbitals, between the active orbitals and within the virtual orbitals for a CAS. The derivation of the working equations of the SSMRPT method is by and large independent of the actual choice of H_0. From the structural nature of the cluster finding equations, it is found that the theory is free from the convergence difficulty due to the intruder states as long as the zero-order energy of the target state is well separated from the unperturbed energy of any

DOI: 10.1021/acs.jpca.6b03211
J. Phys. Chem. A 2016, 120, 5897−5916

virtual function. This also holds good even if some of the $E_{0,\mu\mu}$s are close to $E_{0,ll}$. Consequently, SSMRPT avoids intruders in a natural manner without invoking arbitrary shifting parameters in the denominator. In other words, the stability of the denominators in SSMRPT method within the frame of RSPT in the presence of intruders is quite evident due to the difference between uncorrelated excited state energy and the (nondynamically) correlated ground-state energy. The coupling term, $H_{\mu\nu}$ in eq 2, serves a dual benefit: (i) it yields an intruder-free formulation and (ii) it provides the vital connectivity of the working equations via its simultaneous dependence on both ϕ_μ and ϕ_ν. This connectivity eventually leads to the size-extensivity of the SSMRPT method. In addition, the coupling term becomes overall second-order owing to the presence of $H_{\mu\nu}$ in it. As have been pointed out by Mukherjee and co-workers[32] earlier in the context of the development of the SSMRPT method, we too discard the order argument in favor of size-extensivity.

eq 2 is a coupled equation of $[c_\mu, t_\mu]$ that must be estimated self-consistently. Having determined the amplitudes, the nonsymmetric effective Hamiltonian (describes reference specific dressed Hamiltonian) has been constructed up to order two as $\tilde{H}^{(2)}_{\mu\nu} = H_{\mu\nu} + \sum_l H_{\mu L} t^{l(1)}_\nu(\nu)$. The eigenvalue equation of $\tilde{H}^{(2)}_{\mu\nu}$ yields the energy and the relaxed coefficients of SSMRPT at order 2:

$$\sum_\nu \tilde{H}^{(2)}_{\mu\nu} c_\nu = E^{(2)} c_\mu \tag{3}$$

Although the solution of the first-order cluster amplitudes is carried out with unrelaxed CASSCF coefficients, c^0_ν, the second-order energy contains higher order contributions because of the relaxation of the coefficients due to diagonalization.

In an alternative approach, which is computationally much more affordable, one keeps only frozen coefficients to compute (pesudo) second-order energy: $\langle E^{(2)} \rangle = \sum_{\mu\nu} c^{(0)}_\mu \tilde{H}^{(2)}_{\mu\nu} c^{(0)}_\nu$. This is the unrelaxed description of the SSMRPT method, akin to CASPT2 and MRMP2. Throughout this paper, we have chosen the relaxed description of the method. The major drawback of the SSMRPT approach with CASSCF and IVO-CASCI reference space is its noninvariance with respect to the choice of the reference determinant (as that of the JM-based MR methods) despite the invariance of the zeroth order CAS function, and thus, for noninteracting fragments, the energy is additively separable to the sum of fragment energies if the active orbitals are localized on the asymptotic fragments. Noninvariance of multiexponential JM ansatz based MRCC or MRPT methods with respect to the rotation of active orbitals which are partially occupied in all reference determinants emerges from the noninvariance of the correlated function in an approximate scheme which can be attributed to the lack of invariance of the model functions under the rotation of active orbitals leading to the model function dependence of the amplitudes corresponding to the reference specific cluster operators T_μ. Therefore, to alleviate or at least to attenuate this obvious problem associated with such strategies, one needs to suitably localize the active orbitals on the dissociating fragments in order to preserve the much desired trait of size-consistency. Such a localization has the ability to ensure that in the regime of molecular dissociation, each active orbital lies hinged totally on one fragment, provided that the basic mean field description yields a size-consistent result in the limit of molecular dissociation. The NEVPT2 is also size-consistent with localized orbitals because of the lack of orbital invariance. A very small value of coefficient c_μ of the reference function may lead to rather large values for the cluster amplitudes due to the presence of (c^0_ν/c^0_μ) in the coupling of eq 2, which in turn introduces instability in the effective Hamiltonian and hence in the computed energy. The situation becomes very severe for the CAS of larger dimension, as then many c^0_μ's are close to zero at one point of the potential energy surface of curve(PES/PEC) or another. The simplest solution is to drop every c_μ falling below a threshold in magnitude (less than $\sim 10^{-6}$) and zero the corresponding cluster amplitudes. A more physically appealing solution is to use Tikhonov regularization.[77] At this point, we should mention the recent work of Szabados.[78] It should be noted that for the excited states, the SSMRPT approach often fails to converge. It usually requires more iterations than does the ground state calculation and, in some cases, only an "approximate convergence", using a weaker threshold, can be achieved.

To get rid of the potential singularity problem in the SSMRPT amplitude equations, one can rewrite the working equation in such a manner that the division by c_μs can be minimized to the extent possible. In the unrelaxed SSMRPT variant, the appearance of c_μ in the numerator can be completely circumvented by modifying the cluster finding equation, eq 2, in terms of $x^{l(1)}_\mu(\mu) = t^{l(1)}_\mu(\mu) c^0_\mu$:

$$x^{l(1)}_\mu(\mu) = \frac{H_{l\mu} c^0_\mu + \sum_\nu^{\nu\neq\mu} x^{l(1)}_\mu(\nu) H_{\mu\nu}}{(E_{\mathrm{CAS}} - H_{\mu\mu}) + (E_{0,\mu\mu} - E_{0,ll})} \tag{4}$$

The corresponding energy expression is as follows:

$$\begin{aligned}\langle E^{(2)} \rangle &= \sum_{\mu,\nu} c^{(0)}_\mu \tilde{H}^{(2)}_{\mu\nu} c^{(0)}_\nu \\ &= E_{\mathrm{CAS}} + \sum_{\mu,\nu} c^{(0)}_\nu H_{\nu l} x^{l(1)}_\mu(\mu)\end{aligned} \tag{5}$$

There is no unique definition for the zeroth-order Hamiltonian in a MR framework. The efficacy of a perturbative method depends on the choice of the unperturbed Hamiltonian. In the present paper we have used H_0 operator (monoelectronic in nature) as $H^\mu_0 = \sum_i f_\mu{}^{ii}\{E^i_i\}$ with the following Fock operator:[32]

$$f_\mu = \sum_{ij}\left[f^{ij}_{\mathrm{core}} + \sum_u \left(V^{ju}_{iu} - \frac{1}{2}V^{uj}_{iu}\right) D^\mu_{uu}\right]\{E^j_i\} \tag{6}$$

Here u stands both for a doubly and for a singly occupied active orbital in ϕ_μ, and D^μs are the densities characterized by the active orbitals. In our present work, we want to use the partitioning as close to the MP partitioning in single reference theory as possible in a multipartitioning framework (multi-partitioning MP scheme). We use here a reference dependent multipartitioning scheme first suggested by Zaitsevskii and Malrieu,[79] where for each model function ϕ_μ, the corresponding unperturbed Hamiltonian is chosen as dependent on ϕ_μ.

II.B. Generation of IVO-CASCI Orbitals. The following is a succinct recapitulation of the essential issues of IVO-CASCI method. It is noteworthy that in IVO-CASCI, the virtual orbitals are optimized to efficiently describe the low-lying excited states of the system, and the HF occupied orbitals remain unchanged. Unlike the traditional (HF) treatments in which the orbital and orbital energies are determined from a single Fock operator, the IVO-CASCI method uses multiple Fock operators to define the valence orbitals[41,42] and orbital

DOI: 10.1021/acs.jpca.6b03211
J. Phys. Chem. A 2016, 120, 5897−5916

energies from V^{N-1} potentials, where N is the number of electrons present in the reference HF function. Therefore, the IVOs treat all valence orbitals on an equal footing. The use of IVO-CASCI orbitals as an approximation to CASSCF can be immediately visualized instead of HF. In comparison to HF-based CASCI method, the IVO-CASCI approach circumvents potential difficulties around HOMO−LUMO near degeneracies.

Note if the ground state of the system used is closed shell in nature, one can use the corresponding HF orbitals: $\Phi_0 = \mathcal{A}[\phi_1\overline{\phi}_1\phi_2\overline{\phi}_2\cdots\phi_n\overline{\phi}_n]$ where $\mathcal{A}$ is the antisymmetrizer. Here, i, j, k,⋯ and u, v, w,⋯ characterize the occupied and unoccupied HF molecular orbitals (MOs) respectively. In the IVO-CASCI method, all the MOs are generated via diagonalization of a modified Fock operator constructed from $(N - 1)$ electron potential instead of the normal HF scheme:

$$ {}^{1}F_{lm} = \langle \phi_l | H_1 + \sum_{k=1}^{occ} (2J_k - K_k) | \phi_m \rangle = \delta_{lm}\epsilon_l \tag{7} $$

where l and m stand for any (occupied or unoccupied) HF orbitals and ϵ_l is the corresponding HF energy. H_1 is the one-electron Hamiltonian, and J_k and K_k are Coulomb and exchange operators, respectively, for the occupied Hartree−Fock (HF) molecular orbitals (MOs), e.g., ϕ_k.

The formation of IVOs can be viewed as a single eigenvalue equation of the form: $F'C = C\Gamma$ and the one-body operator F' can be described as follows:

$$ F'_{vw} = {}^{1}F_{vw} + A^{\alpha}_{vw} \tag{8} $$

where ${}^{1}F$ is the ground state Fock operator, and the additional term A^{α}_{vw} (describes the excitation of an electron out of occupied orbital ϕ_{α}) can be defined as follows:

$$ A^{\alpha}_{vw} = \langle \chi_v | - J_\alpha + K_\alpha \pm K_\alpha | \chi_w \rangle \tag{9} $$

In the above equation, the minus and plus signs stand for the triplet (${}^{3}\Psi_{\alpha\rightarrow\mu}$) and singlet (${}^{1}\Psi_{\alpha\rightarrow\mu}$) states, respectively. The corresponding transition energy can be expressed in compact notation in terms of the HF ground state energy, E_{HF} and the eigenvalue of $F'C{=}{=}C\Gamma$ for the μth orbital as

$$ {}^{1,3}\Delta E(\alpha \rightarrow \mu) = E_{HF} + \gamma_\mu - {}^{1}F_{\alpha\alpha} \tag{10} $$

Special care is required for systems where the highest occupied HF MOs are doubly degenerate. In order that the $\{\chi_l\}$s retain molecular symmetry, the construction of F' must be modified from Huzinaga's scheme.[80] If ϕ_α and ϕ_β are the highest occupied degenerate HF MOs, then the matrix element A^{α}_{vw} in eq 9 is replaced for these degenerate systems by $A^{\alpha\beta}_{vw}$, where

$$ A^{\alpha\beta}_{vw} = \frac{1}{2}\langle \chi_v | - J_\alpha + K_\alpha \pm K_\alpha | \chi_w \rangle + \frac{1}{2}\langle \chi_v | - J_\beta + K_\beta \pm K_\beta | \chi_w \rangle \tag{11} $$

Note that in the case of CASSCF scheme, the one particle density matrix is the CASSCF density matrix, however, one-particle density matrix is not the HF density matrix in the case of IVO-CASCI scheme as the active space includes some HF virtual orbitals. Because of the absence of convergence problems and the lack of iterations, it is possible to perform IVO-CASCI calculations with larger CASs than are feasible for the CASSCF method. As in the other MRPT methods, the definition of an active space, the choice of active orbitals, and the specification of the zeroth-order Hamiltonian completely determine the perturbation approximation.

In IVO-CASCI scheme, the state energies and the corresponding wave functions are generated by diagonalizing the Hamiltonian matrix in the CI space:

$$ H|\Psi_I\rangle = E|\Psi_I\rangle \tag{12} $$

Depending on the nature of the state of interest, and also relying upon a prefixed energy criterion, the selection of active orbitals in the IVO-CASCI approach is achieved. In an attempt to circumvent or at least to attenuate the problems associated with the convergence of the perturbative series (frequently arise at higher orders), the CAS is constituted of the orbitals (occupied and IVOs) that are close to the Fermi level. The effort required to computationally implement such a strategy stems out of first, generation of the two-electron MO integrals from the corresponding AO integrals involving only the IVOs (equivalent to a partial two-electron AO→ MO integral transformation). This process scales roughly as the number of two-electron integrals required, namely $\frac{[(N_h + N_v)^4 - N_h^4]}{8}$, where N_h and N_v are the number of occupied and virtual orbitals. Second, the roots need to be generated generating by diagonalizing the CASCI matrix. Both the steps are computationally tractable with ease, and are computationally very simple, provided the CAS is restricted to a moderate size and is not too large. Partial AO→ MO transformation can be achieved independently for a spectrum of choices of CAS without even having the need to repeat the initial SCF calculation. This guarantees an extremely efficient procedure in terms of the computational cost in light of the traditional CASSCF approaches which call for new CASSCF treatments for each CAS and for each symmetry.

III. RESULTS AND DISCUSSION

Investigations on diradicaloid species of various sizes and character, namely, radicaloids such as methylene (CH_2), benzyne (C_6H_4), pyridyne (C_5NH_3), and pyridynium cation ($C_5NH_4^+$) are widely used probing grounds to judge the utility of method(s) tailored to treat static and dynamic correlation simultaneously. We also calculate the PEC and selected spectroscopic constants including bond breaking energy of the lowest three states such as ground state ($X^3\Sigma_g^-$), first (singlet) excited ($a^1\Delta_g$) and second excited ($b^1\Sigma_g^+$) states of the oxygen molecule. In our present work, we have calculated the dissociation energy (which strongly depends on the accuracy of the total energy estimated at a large bond length) by subtracting the energy at a large internuclear separation from that at equilibrium distance. Spectroscopic constants (such as R_e and ω_e) have been computed using a standard sixth order Dunham fit[81] polynomial of the computed PECs. Note that knowledge of bond breaking energies is an important parameter for any analysis of thermodynamic equilibrium constants. As shown in refs 32 and 34−38, the PECs scan with the SSMRPT approach with CASSCF or RHF refernce function can be very successful and accurate results can be obtained. Here, we also critically investigate the performance of our IVO-based variant of SSMRPT method with MP multipartitioning for the evaluation of singlet−triplet splittings of CH_2, and m-benzynes, which have been extensively studied by various theoretical approaches as well as by experimentalists. As these systems are small enough, sufficiently accurate benchmark numbers are available or can be obtained. In the present section, we have

DOI: 10.1021/acs.jpca.6b03211
J. Phys. Chem. A 2016, 120, 5897−5916

evaluated the relative performance of the IVO-SSMRPT *vis-á-vis* other related approaches. We emphasize that although comparison of theoretically calculated values with identical basis sets, active space, and freezing scheme is physically more appealing, in the present paper, for comparison, we have assembled estimates due to different methods with different schemes to get a feeling about the performance and applicability of the present IVO-SSMRPT gradient method. The geometries have been optimized to within a maximum gradient of 10^{-4}.

III.A. 1^1A_1 Methylene (CH_2). The first example concerns CH_2 in $\tilde{a}^1A_1$ (1^1A_1) and $\tilde{c}^1A_1$ (2^1A_1) states for which various excited states are studied in refs 54, 55, and 82−95. Some of its low-lying excited states [e.g., $\tilde{a}^1A_1$ and $\tilde{c}^1A_1$] are said to have diradical character as the two quasi-degenerate orbitals occupied by the unpaired electrons have different symmetries ($3a^1$ and $1b^1$).[2] The ground state methylene, $^3B_1$ CH_2, may be qualitatively described by the configuration: $(1a_1)^2(2a_1)^2(1b_2)^2(3a_1)(1b_1)$. The $\tilde{a}^1A_1$ and $\tilde{c}^1A_1$ excited states are closed-shell singlet and may be described by the admixture two-configuration wave functions [C_{2v} symmetry]: (i) $\phi_1 = (1a_1)^2(2a_1)^2(1b_2)^2(3a_1)^2(2b_1)^0$, and (ii) $\phi_2 = (1a_1)^2(2a_1)^2(1b_2)^2(3a_1)^0(2b_1)^2$. The first excited state, $\tilde{a}^1A_1$, may be appropriately presented by $C_1(1a_1)^2(2a_1)^2(1b_2)^2(3a_1)^2(2b_1)^0 + C_2(1a_1)^2(2a_1)^2(1b_2)^2(3a_1)^0(2b_1)^2$ and the fourth excited state, $\tilde{c}^1A_1$, may be correctly presented by $C_1(1a_1)^2(2a_1)^2(1b_2)^2(3a_1)^0(2b_1)^2 + C_2(1a_1)^2(2a_1)^2(1b_2)^2(3a_1)^2(2b_1)^0$. Note that the CI coefficients $C_1 + C_2$ ($|C_1| > |C_2|$) for the $\tilde{a}^1A_1$ state have opposite signs and the coefficients for the $\tilde{c}^1A_1$ state have the same sign. The $\tilde{c}^1A_1$ state can be viewed as a doubly excited state with respect to the $\tilde{a}^1A_1$ state. To achieve accurate description of these two excited states, both static and dynamic correlation must be treated consistently and accurately.

Here, we constitute the required CAS(2,2) using the configurations ϕ_1 and ϕ_2. We have used DZP and TZ2P basis sets[96] as FCI calculations with these basis sets have already been published by Schaefer III-Sherrill and co-workers.[84,85] We have used the schemes as used in ref.[84,85] In the case of $\tilde{a}^1A_1$ CH_2 state, we also consider cc-pVTZ basis set (with one frozen core orbital) for which a comparison with other multireference CC treatments such as BWMRCCSDT and Mk-MRCCSDT data is available.

Geometrical parameters of $\tilde{a}^1A_1$ CH_2 obtained by various theoretical calculations[54,55,84−87,92,94,97,98] are presented in Table 1 along with experimental values.[99] The values due to IVO-SSMRPT and SS-MRPT level of calculations with DZP and TZ2P basis sets agree very well with each other, and agree with the corresponding FCI results acceptably well, with the deviations (for one frozen core): ΔR_{C-H} (Å)= 0.0094 (0.0087) and $\Delta\angle$H−C−H (deg) = 0.32 (0.44) for IVO-SSMRPT/DZP (SSMRPT/DZP) and ΔR_{C-H} (Å)= 0.0049 (0.0031) and $\Delta\angle$H−C−H (deg) = 0.20 (0.15) for IVO-SSMRPT/TZ2P (CASSCF-SSMRPT/TZ2P). The CCSD(T)-F12x/CBS-(TD)[92] structure for the $\tilde{a}^1A_1$ state is consistent with our structure for the IVO-SSMRPT and SSMRPT methods. Notably, for the cc-pVTZ basis set, the IVO-SSMRPT (and SSMRPT) results are in close agreement with the computationally demanding 2R-RMR-CCSD and 3R-RMR-CCSDT ones.[86,87] As is evident from Table 1, the agreement of IVO-SSMRPT/cc-pVTZ with the Mk-MRCCSDT/cc-pVTZ and BWMRCCSDT/cc-pVTZ estimates is typically in the range of 1−2%. Nevertheless, the computed IVO-SSMRPT (and SSMRPT) and CASPT3 geometrical parameters are in close agreement[94] for the cc-pVTZ basis set. Our IVO-SSMRPT calculations also reproduce the results of MRACPF and MRCI methods.[94] The bond length and angle calculated at IVO-SSMRPT/cc-pVTZ level agree well with the MRCI calculation with d-aug-cc-pCV6Z basis.[94] Finally, we note that on adding carbon 1*s* correlation, using the DZP basis set at the IVO-SSMRPT (and SSMRPT) lower the bond length and angle by 0.0084 and 0.36 (0.0032 and 0.08) respectively with respect to the corresponding frozen core scheme.

The $\tilde{c}^1A_1$ CH_2 is theoretically more challenging than $\tilde{a}$ as it is not the lowest electronic state of its symmetry (second root of its spatial and spin symmetry ($^1A_1$)). Theoretical treatments of such type of states require special attention due to their tendency of variational collapse to the lower-lying state(s). Although the $\tilde{c}$ state of CH_2 is found to be bent at the advanced

Table 1. Results of Equilibrium Geometries (such as Bond Lengths and Angle) for the Closed Shell Singlet (1^1A_1) of the Bent CH_2 System

reference	methods[b,c,d]	R_e (Å)	∠H−C−H (deg)
present work	IVO-SSMRPT/DZP[a]	1.1021	101.40
	CASSCF-SSMRPT/DZP[a]	1.1080	101.80
	IVO-SSMRPT/DZP	1.1105	101.76
	CASSCF-SSMRPT/DZP	1.1112	101.88
	IVO-SSMRPT/TZ2P	1.1040	102.09
	CASSCF-SSMRPT/TZ2P	1.1058	102.04
	IVO-SSMRPT/cc-pVTZ	1.1194	101.68
	CASSCF-SSMRPT/cc-pVTZ	1.1173	101.46
54, 55	SF-SCF/DZP	1.1007	104.05
	SF-CIS(D)/DZP	1.0901	102.70
	SF-OD/DZP	1.1167	102.07
84, 85	TCSCF CISD/DZP	1.1168	101.50
	CCSD(T)/DZP	1.1199	101.28
	CCSDT/DZP	1.1199	101.42
	CISDTQ/DZP	1.1198	101.43
	FCI/DZP	1.1199	101.44
	CCSD(T)/TZ2P	1.1089	101.72
	CCSDT/TZ2P	1.1088	101.86
	FCI/TZ2P	1.1089	101.89
86, 87	SRCCSD/cc-pVDZ	1.127	100.4
	2R-RMR-CCSD/cc-pVDZ	1.127	100.8
	3R-RMR-CCSD/cc-pVDZ	1.127	100.7
	SRCCSD/cc-pVTZ	1.109	101.6
	2R-RMR-CCSD/cc-pVTZ	1.108	101.9
	3R-RMR-CCSD/cc-pVTZ	1.108	101.9
94	CASPT3/cc-pVTZ	1.110	101.5
	MRACPF/cc-pVTZ	1.1107	101.7
	MRCI/cc-pVTZ	1.1190	101.6
	MRCI/d-aug-cc-pCV6Z[a]	1.1061	102.20
92	CCSD(T)/CBS	1.107 99	102.05
	CCSD(T)-F12x/CBS(TD)	1.107 98	102.05
97, 98	Mk-MRCCSDT/cc-pVTZ	1.110	101.90
	BWMRCCSDT/cc-pVTZ	1.110	101.79
99	experiment	1.107	102.4

[a]All-electron calculation. [b]One frozen core orbital: refs 54, 55, 86, 87, 92, and 94. [c]One frozen core orbital: Results of present works with DZP and cc-pVDZ/cc-pVTZ and results of Sherrill and co-workers with DZP basis. [d]One frozen core and one deleted virtual orbitals: Results with TZ2P basis due to the caluclations of SSMRPT, and Sherrill and co-workers.

DOI: 10.1021/acs.jpca.6b03211
J. Phys. Chem. A 2016, 120, 5897−5916

levels of theory used in refs.,[54,55,84−87,91−94] the energy difference between the linear and bent forms is only about 10−20 cm^{-1}. Schaefer, Sherrill, and co-workers[84,85] found the bent structure to be more stable than the linear at all levels considered. It might be difficult to establish the shape of the potential from the experiment. The IVO-CASCI(2,2)-based SSMRPT results for $\tilde{c}^1A_1$ CH_2 are illustrated in Table 2. Akin to

Table 2. Results of Equilibrium Geometries for the ($\tilde{c}^1A_1$) Excited State of the CH_2 System, Where Bond Lengths and Bond Angles Are Given in Å and deg, Respectively

ref	methods[a,b]	R_{C-H}	∠HCH
present work	IVO-SSMRPT/DZP	1.0738	171.86
	CASSCF-SSMRPT/DZP	1.0730	171.48
	IVO-SSMRPT/TZ2P	1.0634	171.09
	CASSCF-SSMRPT/TZ2P	1.0646	171.02
84, 85	TCSCF-CISD/DZP	1.0719	170.00
	FCI/DZP	1.0749	169.68
	TCSCF/TZ2P	1.0556	176.20
	FCI/TZ2P	1.0678	170.08
	TCSCF-CISD/TZ3P(2f,2d)+2diff	1.064	171.6
94	CASPT3/cc-pVTZ	1.068	173.9
	MRACPF/cc-pVTZ	1.068	171.3
	MRCI/cc-pVTZ	1.066	173.9
	MRCI/d-aug-cc-pCV6Z	1.0657	171.92
82, 83	ICMRCI/aug-ccpV5Z	1.068	171.9
100	IC-MR-ACPF/aug-cc-pCVQZ	1.0671	171.89
95	IC-MRCISD+Q/aug-cc-pCVQZ	1.0679	172.0

[a]One frozen core orbital: Results of present works with DZP and cc-pVDZ/cc-pVTZ and results of Sherrill and co-workers with DZP basis. [b]One frozen core and one deleted virtual orbitals: Results with TZ2P basis due to the calculations SSMRPT, and Sherrill and co-workers.

our previous observation for $\tilde{a}$ state, the performance of the IVO-SSMRPT is very similar to the parent CASSCF-SSMRPT one. There are no significant deviations as compared to the FCI results in the general trend of the results for both DZP and TZ2P basis sets in either IVO-SSMRPT or SSMRPT schemes as is evident from the data shown in Table 2. From the table, it is found that the IVO-SSMRPT(SSMRPT) method with DZP basis shows a deviation of the order of ΔR_{C-H} (Å)= 0.0094 (0.0087) and ∆∠H−C−H (deg) = 0.32(0.44). Use of the IVO-SSMRPT/TZ2P [SSMRPT/TZ2P] scheme shows an almost identical deviation pattern: ΔR_{C-H} (Å)= 0.0049 (0.0031) and ∆∠H−C−H (deg) = 0.20(0.15). The computed bond length is in very good agreement with the CASPT3 data. We may conclude that the relative performance of our IVO-SSMRPT (and SSMRPT) is pretty close to the IC-MRCI, IC-MRACPF,[100] and MRACPF[94] values.

The estimation of the singlet−triplet separation (ΔE_{ST}) of CH_2 can be used to assess the accuracy of theoretical methods as it requires a precise and well-balanced incorporation of electron correlation effects and an accurate description of the ground and excited states of different symmetries and multiplicities. The calculation of E_{ST} is important for its reactivity and specificity as reaction intermediates. Indeed, calculations and experiments both find the triplet to be the ground state of CH_2. To compute ΔE_{ST}, we use the same FCI geometries and scheme as in refs 84 and 85 for both DZP and TZ2P basis sets. The excitation energies obtained with IVO-SSMRPT and CASSCF-SSMRPT methods are compared with previous calculations in Table 3. From the results, it can be

Table 3. Adiabatic Singlet−Triplet Energy of CH_2 (the Energy Difference between the E^1A_1 and E^3B_1 States)[a]

reference	methods	ΔE_{ST} (kcal/mol)
present work	IVO-SSMRPT/DZP	16.10
	CASSCF-SSMRPT/DZP	15.45
	IVO-SSMRPT/TZ2P	16.22
	CASSCF-SSMRPT/TZ2P	15.65
68, 88	CASPT2/DZP	15.44
	CASPT3/DZP	12.80
	MRCI/DZP	11.92
93	GVVPT2/DZP	15.38
	SDS-MSMRPT2/DZP	12.49
	MRCISD/DZP	12.00
18, 19	SC-NEVPT2/DZP	13.67
	PC-NEVPT2/DZP	13.52
	SC-NEVPT/DZP	13.01
89, 90	CR-CCSD(T)/DZP	12.41
	CR-CC(2,3)/DZP	12.41
	CCSDt/TZP	11.68
	CC(t;3)/TZP	11.3
	CCSDT/TZP	11.25
84, 85	FCI/DZP	11.14
68, 88	CASPT2-F12/cc-VDZ-F12	12.67
	CASPT2/cc-VDZ-F12	14.19
	CASPT2 CBS	12.8
54, 55	SF-CIS(D)/cc-pVDZ	14.18
	SF-OD/cc-pVDZ	12.08
101	VMC/JSD/ECP	13.45
	LRDMC/JSD/ECP	13.36
91	CAS-BCCC4/cc-pVDZ	11.37
	CAS-BCCC4/cc-pVQZ	9.18
86, 87	SU-MRCCSD/cc-pVDZ	12.04
	SU-MRCCSD(T)/cc-pVDZ	12.20
103	DEA-EOM-CCSD/cc-pVDZ	11.6
	DEA-STEOM-CCSD/cc-pVDZ	14.0
	ΛCCSD(T)/cc-pVDZ	12.1
	CCSDT/cc-pVDZ	11.8
102	experiment	8.998

[a]NEVPT2, CASPT2 and CASPT2-F12 calculations usees the full-valence active space.

concluded that all the methods considered here overestimate the singlet−triplet gaps. As in the case of geometrical parameters, CASSCF-SSMRPT agrees very well with IVO-SSMRPT. The estimated energy gap obtained by the variational Monte Carlo (VMC/JSD/ECP) and the lattice regularized diffusion Monte Carlo (LRDMC/JSD/ECP) are 13.45 and 13.36 kcal/mol, respectively,[101] which are also in good accordance with our present estimated energy gaps. Our estimated gaps are also in very good agreement with the experimentally derived data of 9.363 kcal/mol.[102] It is worth noting that the values obtained for the Jastrow correlated single Slater determinant VMC/ECP and LRDMC/ECP are 8.09 and 8.58 kcal/mol, respectively.[101] The experimental measurement for ΔE_{TS} without considering the relativistic and nonadiabatic effects provides a value of 8.998 kcal/mol.[102] The values of energy gap due to IVO-SSMRPT and SSMRPT are generally in very close agreement with the GVVPT2, CASPT2, and NEVPT2 values for DZP. The IVO-SSMRPT/DZP (SSMRPT/DZP) excitation energy is found to be almost 5 (4) kcal/mol higher than the FCI/DZP value. The corresponding deviations in the cases of CASPT2/DZP and

DOI: 10.1021/acs.jpca.6b03211
J. Phys. Chem. A 2016, 120, 5897−5916

NEVPT2/DZP are around 4 and 2 kcal/mol, respectively. As seen in the table, the IVO-SSMRPT values with CAS(2,2) agree nicely with the CASPT2-F12 and CASPT2/CBS results with full-valence active space. Both the CR-CCSD(T) [completely renormalized CCSD(T)] and CR-CC(2,3) [completely renormalized CC approach with singles, doubles, and noniterative triples] predicted splittings agree with IVO-SSMRP (and SSMRPT) to within a few kcal/mol. There is also good agreement of IVO-SSMRPT/cc-pVDZ with the SF-CIS(D)/cc-pVDZ and SF-OD/cc-pVDZ results.[54,55] The good agreement of IVO-SSMRPT (and SSMRPT) with the current generation computationally expensive *state-of-the-art* calculations such as BCCC4 [block-correlated CC truncated to the four-block correlation level], SU-MRCC [state-universal MRCC], CR-CC, CC(t;3), CCSDt, CCSD(T), CCSDT, ΛCCSD, and DIP-EOM-CCSD computations[103] methods attest the reliability of a properly constructed IVO-SSMRPT as well as SSMRPT/CASSCF wave functions. The use of larger active spaces in association with larger basis sets can enhance the accurateness of the computed values.

Next, we focus on the application of gradient IVO-SSMRPT method to the geometry optimizations for the lowest singlet states of aryne compounds such as *m*-benzyne, and the 2,6-isomers of pyridyne (didehydropyridine) and the pyridynium cation [shown in Figure 1] which serve as probing grounds for

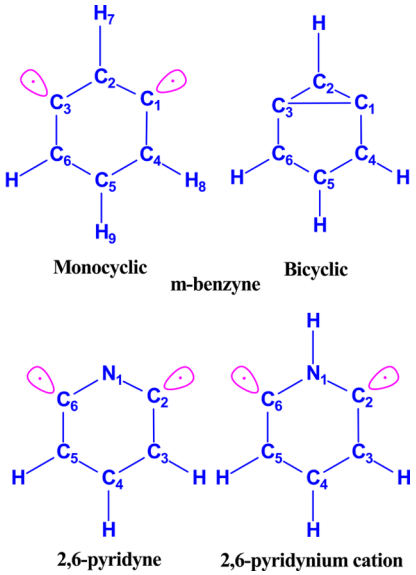

Figure 1. Structures of *m*-benzyne, 2,6-pyridyne, and 2,6-pyridynium cation.

various MR approaches as their biradical character (depending on the distance between the two radical centers)[1] requires a correct and balanced description of dynamic and nondynamic correlation effects if accurate energies and structures are to be estimated. Biradicals are highly reactive species and are of great interest for organic chemists and biochemists. The quasidegenerate nature of the monocyclic form of these systems is clearly evident from the values of the reference coefficients mentioned in Table 4 in refs 104 and 105. Note that both 2,6-isomers of pyridyne and the pyridynium cation formally emerge from *m*-benzyne by replacing the C1 carbon atom by either a N atom or a NH group. These biradicals share a similar electronic structure governed by the pair of frontier orbitals. It is worth noting that the active orbitals of 2,6- isomers of pyridyne and pyridynium cation are of similar shape as that of *m*-benzyne.[104,105] Both *m*-benzyne and 2,6-pyridyne are particularly interesting as they may potentially exist as monocyclic or bicyclic compounds. For all three aryne systems considered here, two closed-shell configurations are used as reference functions [i.e., CAS(2,2)] with orbitals taken either from IVO-CASCI or from CASSCF within the framework of C_{2v} symmetry. The two active orbitals a_1 and b_2 involved in the two model functions belong to different symmetries. This is the physically motivated optimally correct zero order description of the systems. The correlation-consistent, core−valence polarized basis set, cc-pCVTZ, of Woon and Dunning[106] have been employed in our computations and all electrons were correlated. For these systems, here, we use Mk-MRCC values (with orbitals taken either from RHF or from TCSCF calculations) as reference data.[104,105,107,108]

III.B. Singlet *meta*-Benzyne (C_6H_4). *m*-benzyne (1,3-didehydrobenzene), the middle child of the benzyne family, is indeed infamous for its computational challenges.[33,104,105,109−122] The previous MCSCF level of geometry optimization predicts that the monocyclic structure is more stable with respect to the bicyclic one by amount 12.9 kcal/mol,[115,116] whereas the RHF investigation favors the bicyclic one over the monocyclic form by about 18 kcal/mol. Note that the fixed-node diffusion Monte Carlo (DMC) studies based on CAS(8,8) demonstrate that the monocyclic form is lower in energy than the bicyclic one by 1.9 kcal/mol[123] which is in agreement with the previously published high level CC estimates due to Smith et al.[121] Kraka et al.[115,116] stated that the energy surface is very flat along the C1−C3 coordinate for *m*-benzyne, nevertheless around ∼5 kcal/mol[115,116] is required to recouple the electrons to a closed-shell singlet electron pair required for the formation of a 1,3 C−C bond. According to the analysis of Sander et al.,[110−112] *m*-benzyne is not even a minimum on the C_6H_4 energy surface.

Table 4 summarizes IVO-SSMRPT predictions of the structure of *m*-benzyne. For the system *m*-benzyne, we have also performed CASSCF (8,8) and IVO-CASSCF (8,8) computations, prior to performing the corresponding SSMRPT with these as reference spaces. The results corresponding to these are enunciated in Table 1 in ref 124. However, we envisage that the results do not show perceptible improvement when compared to those of the same with CASSCF(2,2) and IVO-CASSCF(2,2). In view of this, we rely upon the smaller CAS and perform our perturbative calculations with the same. This additionally brings onto fore the fact that our method is effective enough in handling strongly correlated systems even with small active spaces as compared to other perturbative techniques that rely on larger CAS. The present work and other theoretical studies mentioned in the table have revealed that the ground state of *m*-benzyne is biradical monocyclic. Reliable CCSD(T), CAS(8,8)CISD+Q, and CASPT2 calculations also refute the claim of bicyclic structure of *m*- benzyne.[110−112] Jagau and Gauss[104,105] state that the MR-AQCC/cc-pCVDZ calculations predict a monocyclic structure with C1−C3 distance of 2.13747 Å. Present IVO-SSMRPT/cc-pVTZ calculations clearly indicate a monocyclic form as a possible structure for the *m*-benzynes [with C1−C3 distance and ∠C1−C2−C3 of 1.8932 Å and 89.60°, respectively]. The SSMRPT with CASSCF(2,2) orbitals computation concur that the system has a singlet ground state with a monocyclic structure (rather than the incorrect closed-shell bicyclic structure) which has C1−C3 = 1.8832 Å and ∠C1−C2−C3 = 87.00°. Moreover,

DOI: 10.1021/acs.jpca.6b03211
J. Phys. Chem. A 2016, 120, 5897−5916

Table 4. Structural Parameters of the Ground State of *m*-Benzyne.[a] Bond Lengths Are Given in Å and Bond Angles Are Given in Degree (°). Values Enclosed in Parentheses Due To the Mk-MRCCSD Level of Theory Using the TCSCF-Orbitals.

parameters	CCSD[b]	CCSD(T)[b]	Mk-MRPT2[b]	BWP91[c]	CASPT2[d]	REKS[e]	Mk-MRCCSD[f]	SSMRPT	IVO-SSMRPT
basis	(cc-pVTZ)	(cc-pVTZ)	(cc-pVTZ)	(cc-pVDZ)	(ANO-L)	(6-31G(d))	(cc-pCVTZ)	(cc-pVTZ)	(cc-pVTZ)
C1−*C2*	1.3485	1.3717	1.3539	1.365	1.367	1.394	1.3586 (1.3594)	1.3611	1.3429
C1−*C4*	1.3820	1.3785	1.3721	1.382	1.368	1.383	1.3697 (1.3696)	1.3681	1.3690
C4−*C5*	1.4092	1.4031	1.4009	1.411	1.397	1.415	1.3945 (1.3954)	1.4082	1.4007
C1−*C3*	1.5635	2.0581	1.8726	1.874	2.074	2.083	2.5506 (2.5459)	1.8823	1.8932
C2−*H7*	1.0796	1.0775	1.0777			1.091	1.0745 (1.0748)	1.0768	1.0745
C4−*H8*	1.0771	1.0821	1.0799				1.0789 (1.0788)	1.0817	1.0801
C5−*H9*	1.0838	1.0862	1.0848			1.099	1.0825 (1.0827)	1.0831	1.0811
∠C1−C2−C3	70.87	97.2	87.5		98.7	96.7	94.65 (95.60)	87.00	89.60
∠C2−C3−C6	160.75	137.49	145.64		136.3	138.1	139.66 (138.91)	145.70	144.64
∠C3−C6−C5	107.91	117.00	114.70		117.4	116.8	116.32 (116.49)	117.07	117.10
∠C6−C5−C4	111.8	113.8	111.8		113.9	113.6	113.39 (113.61)	113.40	112.82

[a]In the CASPT2 calculations, CAS(12,12) have been used. Note that the CAS used in the CASPT2 calculation are larger than ours CAS(2,2). [b]Reference 33. [c]Reference 113. [d]Reference 122. [e]References 115 and 116. [f]References 104 and 105.

Mk-MRPT2/cc-pVTZ calculations[33] also support our structural parameters, in which the C1−C3 bond length and C1−C2−C3 angle are 1.8726 Å and 87.50°, respectively. The C1−C3 values provided by the present IVO-SSMRPT and Mk-MRPT2[33] calculations are somewhat smaller than the SSMRPT distance. Note that the relaxed version of Mk-MRPT2[33] provide the C1−C3 distance as 1.997 Åwhich is very close to our present IVO-SSMRPT estimates. Note that the full-blown Mk-MRCCSD/cc-pCVTZ gradient calculations yield the monocyclic structure [C1−C3 = 2.5506 (2.5459) Å and ∠C1−C2−C3 = 139.66° (138.91°) for RHF (TCSCF) orbitals] rather than a bicyclic form. The bond distances and angles of *m*-benzyne due to our IVO-SSMRPT and SSMRPT calculations are very close to the ones obtained by Jagau et al.[104,105] at the Mk-MRCCSD/cc-pCVTZ level of theory for both RHF and TCSCF orbitals (SSMRPT calculations use much less CPU time than MK-MRCCSD theory). IVO-SSMRPT study also agree with the findings of Shaik et al.,[115,116] namely that the REKS(2,2)/6-31G(d,p) [spin-restricted ensemble-referenced Kohn−Sham][115,116] geometry is monocyclic with C1−C3 = 2.083 Å and ∠C1−C2−C3 = 96.7°. Extensive analytic energy gradient CC study on *m*-benzyne with various basis sets in conjunction with different orbitals [e.g., spin restricted, spin-unrestricted, and Bruekner orbitals] due to Smith et al. indicate that CCSD prefers the bicyclic form as the ground state with a C1−C3 bond length of ∼1.551 Å and CCSDT as well as CCSD(T) both methods predict monocyclic form as the stable structure with a C1−C3 bond length of 2.093 and 2.026 Å, respectively. The CCSD(T) level of calculations using an augmented valence triple-ξ basis of the 6-311G(2d,2p) type also favor monocyclic biradical structure with C1−C3 = 2.101.[110−112] These results can be explained in terms of effects emerged from three-electron through-bond delocalization[117,118] for which connected triples are very important for a correct description. The CASPT2(12,12)/cc-pVTZ calculation adopts a monocyclic structure in which the distance of the radical center (C1−C3) is around 2.074 Å and ∠C1−C2−C3 = 98.7°.[122] The overall agreement between the optimized geometrical parameters calculated by the IVO-SSMRPT(2,2) and CASPT2(12,12) methods is quite good. As shown in Table 4, the bond length and angle calculated from the IVO-SSMRPT and SSMRPT methods are in good agreement with previous CCSD(T)[33] estimates for the cc-pvTZ basis set. Note that the broken-symmetry CCSD(T)/6-311++G(2d,2p) produces[103] a geometry in relatively close agreement with our method, thus giving confidence to our estimate. Hess[125] argued that the measured IR spectrum[110−112] of monocyclic form can be equally fitted to the calculated IR spectrum of bicyclic form. In this context we should reiterate the observation of Winkler and Sander.[117,118] They argued (exploiting natural bond-orbital analysis) that the σ-allylic C1−C2−C3 system is the best representation of the monocyclic form of *m*-benzyne as delocalization of the two single electrons occurs through-space and through-bond interactions via the antibonding C2−H7 and the geminal C1−C2 and C2−C3 bonds. Kraka and co-workers[117,118] also mentioned that apart from the quantum chemical evidence, there is also chemical evidence to refute the existence of bicyclic closed-shell structure of *m*-benzyne.

Although the investigations due to CC and MRPT calculations are conclusive about the structure of *m*-benzyne, the structural predictions of DFT are inconclusive, strongly influenced by the approximate exchange-correlation functional used for the calculations.[115−118,126−128] Recent experimental results[129] on the substituted *m*-benzyne suggest that the real structure of *m*-benzyne is closer to the bicyclic form rather than the monocyclic one.

The adiabatic triplet−singlet (TS) gaps (ΔE_{TS}) in the *m*-benzyne obtained by IVO-SSMRPT (without corrections for zero point energy) and other credible computational methods are summarized in Table 5. The large TS splitting suggests that the through-space bonding interaction in *m*-benzyne is substantial and results in a strong preference for a singlet ground state. In our present calculations of ΔE_{TS}, we have performed single-point IVO-SSMRPT calculations using the structural parameters of Evangelista et al.[130] obtained via the RHF-CCSD(T)/cc-pVTZ and ROHF-UCCSD(T)/cc-pVTZ level of theory, respectively. As far as the TS splitting is concerned, Evangelista et al.[130] showed that the basis set dependence of TS-gaps is not significant. Our IVO-SSMRPT method predicts the correct ordering of the lowest singlet and triplet states and gives TS splittings in good agreement with the established theoretical values such as REKS, and CASRS3 (CASSCF-based MR third order perturbation theory). The ΔE_{TS} values[122] obtained by CASPT2 with CASSCF(8,8) and CASSCF(12,12) are in good agreement with IVO-SSMRPT. Furthermore, the IVO-SSMRPT result is at par with CCSD-(T)/cc-pVTZ[86,87] (18.15 versus 18.8 kcal/mol). ΔE_{TS} at the IVO-SSMRPT level of theory is also in good agreement with

DOI: 10.1021/acs.jpca.6b03211
J. Phys. Chem. A 2016, 120, 5897−5916

Table 5. Adiabatic Triplet−Singlet Splitting (in kcal/mol) for *m*-Benzyne

reference	methods	ΔE_{TS} (kcal/mol)[b,c]
present work	IVO-SSMRPT/cc-pVTZ	18.15
	CASSCF-SSMRPT/cc-pVTZ	18.03
	CASSCF(2,2)/cc-pVTZ	11.90
	IVO-CASCI(2,2)/cc-pVTZ	12.05
122	CASPT2(8,8)/ANO-L	20.3
	CASPT2(8,8)/ANO-L	20.3
113	CASPT2/aANO	19.0
	CCSD(T)/pVTZ	20.7
113	CASRS3/CBL(4:3,4)	18.6
86, 87	CCSD(T)/cc-pVTZ[a]	18.8
	CRCC(2,3)/cc-pVTZ[a]	16.4
115, 116	REKS/6-31G(d)E	21.6
119, 120	SF-CCSD/cc-pVTZ	18.03
	SF-CCSD(dT)/cc-pVTZ	20.57
	DEA-EOM-CCSD/cc-pVTZ	18.3
	DIP-EOM-CCSD/cc-PVTZ	19.7
	DEA-STEOMCCSD/cc-PVTZ	15.3
131	icMRCCSD D + CBS + ZPVE	18.2
130	Mk-MRPT2/cc-pVTZ	24.11
	Mk-MRCCSD/cc-pVTZ	20.97
	Mk-MRCCSD+CBS+ZPVE	19.5
	CCSD/cc-pVTZ	9.74
86, 87	RMRCCSD/CCSDb+CBS+ZPVE	15.0
	RMRCCSD(T)/CCSD(T)b+CBS+ZPVE	19.2
	CAS-BCCC4	17.3
132	BHLYP	18.82
	SF50/50	22.30
109	experiment	21.0

[a]Use a modified cc-pVTZ in which the f functions on carbons and the d functions on hydrogens are omitted. [b]The zero-point vibrational energy (ZPVE) correction obtained at the CCSD(T) level is 0.9 kcal/mol.[54,55]. [c]The correction for the complete basis set limit (CBS) for CCSD, plus a ZPVE correction obtained at the CCSD(T) level is 0.8 kcal/mol.[54,55]

the results of computationally demanding SF-CC,[119,120] DEA-EOM-CCSD/cc-pVTZ[103] and DIP-EOM-CCSD/cc-PVTZ[103] methods. Note that ΔE_{TS} value calculated with IVO-SSMRPT is about 0.05, 1.35, and 1.05 kcal/mol lower than the icMRCCSD + CBS + ZPVE, Mk-MRCCSD + CBS + ZPVE, and RMRCCSD(T)/CCSD(T)b + CBS + ZPVE values, respectively. As shown in Table 5, the TS splitting provided by IVO-SSMRPT/cc-pVTZ method is in nice agreement with the CASSCF(2,2)-based BCCC4/cc-pVDZ estimate.[91] Calculated ΔE_{TS} with CAS-BCCC4/cc-pVDZ is about 0.85 kcal/mol lower than the IVO-SSMRPT/cc-pVTZ value. The IVO-SSMRPT result is also in close proximity to the experimental value,[109] the deviations amounting to 3 kcal/mol. However, the calculations with larger basis sets (or the inclusion of higher-order treatment) are still necessary to yield more definitive TS spillitings.[131] At SF-CCSD/cc-pVTZ and SF-CCSD(dT)/cc-pVTZ, Slipchenko and Krylov obtained the values of 18.03 and 20.57 kcal/mol respectively, which are 3 and 0.4 kcal/mol larger than experimental results, respectively. The computed splittings via CR-CC(2,3) and DEA-STEOMCCSD[103] calculations[86,87] are least satisfactory in this regard, a rather large deviation from experimental data of about 4.6 and 5.7 kcal/mol, respectively are found. The TS splitting obtained using IVO-SSMRPT is also in accordance with the spin-flip TD-DFT method.[132] As the TS energy splitting is an important gauge in the study of reactivity of the diradicals in DNA cleavage, IVO-SSMRPT like other established quantum chemistry methods has potential to be a routine low-cost method for investigating the reactions.

C. Singlet 2,6-Pyridyne (C_5NH_3). The 2,6-isomer of didehydropyridine (pyridyne) exhibits strong biradical character and thus its theoretical treatment remains a challenge until today.[104,105,107,108,127,133,134] Via this study we have also examined the effect of heteroatom incorporation into the *m*-benzyne. Introducing a nitrogen atom into the aromatic ring perturbs the structure and energy of the benzyne. As that of *m*-benzyne, a particularly intriguing aspect of 2,6-pyridyne is the possibility that it may exist as monocyclic or bicyclic form [monitored by means of the ∠C2−N1−C6 or, alternatively, the C2−C6 distance; see Figure 1]. Although for *m*-benzyne the bicyclic structure can be viewed as an artifact of methods (in its ability to provide a proper description of the MR character in the wave function) used to study, the issue has yet not been fully resolved in the case of the 2,6-pyridyne. While Mk-MRCCSD level of calculation favors the monocyclic form by around 4 kcal/mol, the bicyclic form is found to be more stable for CCSD by about 2 kcal/mol.[107,108] However, when the effect of connected triples are incorporated at the CCSD via CCSD(T) [or CCSDT], the monocyclic form is found to be lower in energy than the bicyclic one by about 5.5 (3.9) kcal/mol.[107,108] This finding illustrates the difficulty associated with the traditional CCSD treatment and provides an argument for

Table 6. Structural Parameters of the Ground State of 2,6-Pyridyne (C_5NH_3)[a]

parameters	CCSD[b]	CCSD(T)[b]	Mk-MRCCSD[b]	R-MRCCSD(T)[c]	B3LYP[d]	CASSCF-SSMRPT	IVO-SSMRPT
N1−C2	1.3313	1.3470	1.3361	1.360	1.337	1.3355	1.3349
C2−C3	1.3734	1.3801	1.3735	1.395	1.380	1.3783	1.3772
C3−C4	1.3936	1.3964	1.3908	1.397	1.411	1.3929	1.4010
C2−C6	1.8184	2.0146	2.0169			2.0434	2.0421
C3−H	1.0771	1.0800	1.0777			1.0772	1.0767
C4−H	1.0838	1.0855	1.0825			1.0808	1.0810
∠C2−N1−C6	86.15	96.80	98.01	100	69	99.82	99.80
∠N1−C2−C3	146.94	138.12	137.45			136.99	136.83
∠C2−C3−C4	114.52	117.01	116.80			116.07	116.00
∠C3−C4−C5	110.93	112.93	113.49	118	111	113.30	113.22
∠C2−C3−H	120.74	119.51	119.78			119.34	119.30

[a]Bond lengths and bond angles are given in Å and deg, respectively. [b]References 107, 108. [c]Reference 134. [d]Reference 127.

DOI: 10.1021/acs.jpca.6b03211
J. Phys. Chem. A 2016, 120, 5897−5916

Table 7. Structural Parameters of the Ground (Singlet) State of 2,6-Pyridynium Cation ($C_5NH_4^+$)[a]

parameters	CCSD[b]	CCSD(T)[b]	Mk-MRCCSD[b]	B3LYP	BPW91[c]	MR-AQCCSD[d]	CASSCF-SSMRPT	IVO-SSMRPT
N1−C2	1.3235	1.3375	1.3292 (1.3293)	1.3291	1.347	1.3459	1.3288	1.3281
C2−C3	1.3570	1.3647	1.3568 (1.3568)	1.3602	1.371	1.3768	1.3627	1.3601
C3−C4	1.3994	1.4041	1.3992 (1.3994)	1.4129		1.4135	1.3975	1.3998
C2−C6	2.1215	2.2036	2.1833 (2.1865)	2.1015	2.242	2.2290	2.1940	2.1867
N1−H	1.0105	1.0129	1.0102 (1.0106)	1.0242		1.0208	1.0087	1.0088
C3−H	1.0788	1.0811	1.0788 (1.0788)	1.0933		1.0921	1.0792	1.0717
C4−H	1.0818	1.0834	1.0807 (1.0814)	1.0955		1.0946	1.0808	1.0800
∠C2−N1−C6	106.54	110.93	110.43 (110.66)	104.47		112.21	111.30	110.82
∠N1−C2−C3	131.94	128.51	129.05 (128.92)	133.59		127.68	128.20	128.07
∠C2−C3−C4	117.02	117.59	117.27 (117.19)	116.88		-	117.88	117.82
∠C3−C4−C5	115.54	116.87	116.94 (117.12)	114.59		-	116.94	116.32
∠C2−C3−H	119.95	119.90	120.12 (120.24)	120.54		120.08	120.02	120.04

[a]Bond lengths and bond angles are given in Å and deg, respectively. Values enclosed in parentheses due to the the Mk-MRCCSD level of theory using the TCSCF-orbitals. [b]Reference 107, 108. [c]Reference.[127] [d]References 104, 105 for cc-pCVDZ.

the consideration of MR-based methods for this purpose. The Mk-MRCCSD(T) favors the monocyclic form by more than 5 kcal/mol with respect to the bicyclic form.[107,108] Note that as HF-SCF calculations, BPW91/cc-pVDZ method leads to a bicyclic structure.

The results obtained with SSMRPT and IVO-SSMRPT methods are summarized in Table 6 for cc-pCVTZ basis. Results assembled in Table 6 illustrate the role played by the MR effects (and also the higher-than-double excitations). The agreement of IVO-SSMRPT and SSMRPT methods with the MR-based CC results considered here is much better than for the values provided by the SR-based CC calculations. For cc-pCVTZ basis, as that of the CCSD(T), CCSDT, Mk-MRCCSD, and Mk-MRCCSD(T) level of calculations, SSMRPT and IVO-SSMRPT methods clearly predict a monocyclic structure with C2−C6 = 2.0434 Å and C2−C6 = 2.0421 Å values, respectively. Although the CCSD/cc-pCVTZ treatment yields the smallest ∠C2−N1−C6 with 86.15°, SSMRPT/cc-pCVTZ and IVO-SSMRPT/cc-pCVTZ along with CCSD(T)/cc-pCVTZ and Mk-MRCCSD/cc-pCVTZ calculations[107,108] yield wider ∠C2−N1−C6 values of 99.82° and 99.80° as well as 96.80° and 98.01°, respectively. Consistent with this finding, CCSD calculations provides a shorter C2−C6 distance (=1.9140 Å) than the SSMRPT and IVO-SSMRPT computations. The CCSD(T) and Mk-MRCCSD calculations in ref.[107,108] provide a larger C2−C6 distances (2.0146 Å and 2.0169 Å, respectively) than CCSD results for cc-pCVTZ basis set. Note that the RMRCCSD(T) treatment yields value for the ∠C2−N1−C6 as 100° which is close to the CASSCF(8,8) value[127] of 106.2°. Note that the C2−C6 distance and ∠C2−N1−C6 are 1.561 Å and 69°, respectively, for BPW91/cc-pVDZ and hence yields a minimum for the bicyclic structure (very different from those predicted at the Mk-MRCCSD/Mk-MRCCSD(T) and SSMRPT/IVO-SSMRPT levels). Finally, we note that the C2−C6 bond length for 2,6-pyridyne estimated using the EOMSF-CCSD/6-31G* level of theory (2.084 Å) display the same pattern as our results.[104,105]

D. Singlet 2,6-Pyridynium Cation. To explore the electronic structure of didehydropyridinium or pyridynium cation [$C_5NH_4^+$] various calculations have been performed using density functional theory and wave function-based methods.[87,104,105,107,108,127,133,134] A concluding assessment of the optimized structures is difficult due to the lack of reliable reference (experimental) data. Mk-MRCC results[107,108] on this charged system have been used as a reference to gauge the applicability of our IVO-SSMRPT gradient calculation. The single reference mean-field, e.g., HF, level of calculation provides the incorrect closed-shell bicyclic structure (with C2−C6 distance about 1.5 Å), while by incorporation of nondynamical correlation using MR mean field calculation via CASSCF, the bicyclic structures inevitably open to monocyclic ones.[107,108] Various advanced theoretical calculations[87,104,105,107,108,127,133,134] lead to a monocyclic form for this system.

The optimized geometries as obtained in the CAS(2,2)-based IVO-SSMRPT and SSMRPT calculations with the cc-pCVTZ basis set are given in Table 7 together with results computed from other methods. Table 7 shows that SSMRPT calculations with IVO-CASCI and CASSCF orbitals lead to overall consistent geometrical parameters for the 2,6 pyridynium cation, which agree quantitatively with the Mk-MRCCSD results for the singlet state. All calculations mentioned here attribute a longer C2−C6 distance. The table points out the fact that, akin to the CCSD [with C2−C6= 2.1215 Å], CCSD(T) [with C2−C6 = 2.2036 Å]), and Mk-MRCCSD [with C2−C6 = 2.1833 Å] methods, the SS-MRMPPT and IVO-SSMRPT gradient too provides the open-shell monocyclic structure with a C2−C6 distance of 2.1940 and 2.1867 Å, respectively. EOMEE-CCSD calculation[104,105] also yields the monocyclic structure with a long C2−C6 distance of 2.15 Å. Prochnow et al.[107,108] argued that the variation of the C2−C6 distance due to the correction of connected triples is rather significant and hence renders the CCSD values questionable. In contrast to *m*-benzyne, DFT optimization schemes (via B3LYP and BPW91 methods) correctly predict the monocyclic form of pyridynium cation as being the more stable one with C2−C6 = 2.2 Å. It is seen that the IVO-SSMRPT and SSMRPT gradient methods perform very close to MR-AQCC method of Jagau-Gauss.[104,105]

The present calculations clearly demonstrate that the ground and excited electronic structure of the radicaloids species mentioned above are well represented by the SSMRPT method with a IVO-CASCI reference function constructed over SCF orbitals. The optimized geometries provided in the present work confirm that the use of IVO-CASCI orbitals instead of CASSCF ones in the SSMRPT calculations do not distinctly change the investigated structural parameters for C_6H_4, C_5NH_3 and $C_5NH_4^+$ molecules examined. The comparison between the values for the C2−C6 distance obtained using IVO-CASCI-

DOI: 10.1021/acs.jpca.6b03211
J. Phys. Chem. A 2016, 120, 5897−5916

(2,2) orbitals and those obtained using CASSCF(2,2) orbitals displays differences of about 0.186 Å for C_6H_4 while for C_5NH_3 and $C_5NH_4^+$ the shift of the C2−C6 distance is about 0.001 and 0.007 Å, respectively. In addition, both the IVO-SSMRPT and CASSCF-SSMRPT estimates exhibit reasonable agreement with the available experimental results.

The most exacting assessment of any approach tailored to handle quasy-degeneracy is by computing the dissociation surfaces/curves of molecules for which a single reference method is poorly suited. It should be noted that in the bond dissociation process, the degree of quasi-degeneracy can be varied continuously from a nondegenerate situation to a highly degenerate one as the bond is stretched/compressed. Profiling a PEC thus needs a MR description and the maintenance of size-extensivity. The PEC plays an important role in the description, simulation, and modeling of molecular systems. Hence, the present study on double bond dissociation of O_2 is very useful to test the applicability of our method.

E. Molecular Oxygen, O_2. For O_2 molecule, the ground state, $X^3\Sigma_g^-$ has a single reference character whereas the first two excited states $a^1\Delta_g$ and $b^1\Sigma_g^+$ have significant MR character. The breaking of $X^3\Sigma_g^-$ O_2 into two (triplet) oxygen atoms is a archetypal example of open-shell systems. The two orbitals, π_{2p_x} and π_{2p_y}, contain an unpaired electron each with the same spin and constitute the ground electronic state, $X^3\Sigma_g^-$. Two possible singlet excited states stem out as a consequence of the rearrangement of the electron spins within these two degenerate orbitals. The two unpaired electrons of the $a^1\Delta_g$ occupy the same MO, with an option of two MOs that these two electrons can occupy. The singlet state $b^1\Sigma_g^+$ has two unpaired and antiparallel electrons. Therefore, MR computations improve the description of these two excited states. The nontrivial behavior of the oxygen molecule (stem from the interaction of unpaired electrons), exhibiting thermodynamic reactivity but kinetic tendency of not to react, is borne out of the fact that the molecule has a triplet ground state that prohibits its spin-forbidden reaction with singlet-state molecules, and such transformations are seen to occur very slowly at room temperatures. It is seen that both the singlet excited states are appreciably reactive, and particularly, the reactivity of the first excited state has a direct relevance in biology. Many of the biological molecules like the DNA, proteins and lipids are known to react with the singlet oxygen due to its cytotoxic properties. This necessitates a thorough exploration of the physicochemical nature of the lowest-lying excited states of oxygen. Thus, one looks forward to theoretically explore the PEC of the low-lying electronic states of O_2 in an attempt to gain a deeper insight into the phenomenon. Various methods have already been employed to study O_2 in its ground and excited states.[135−144] Throughout the calculations we have used the same basis, double-ζ plus polarization (DZP) and scheme as used by Bauschicher and Langhoff.[135] Although the basis set is small [and hence FCI are available[135]], we can exploit it to make various interesting observations to illustrate the utility of the IVO-SSMRPT method in vogue. Keeping in mind the scheme of Bauschicher and Langhoff,[135] we have also used the frozen core FCI values at some other geometries for both the states considered here.[140] It is worth mentioning that the complete FCI PEC results are not available even with DZP basis set. Here, we have considered CAS(8,6), eight electrons are distributed in six active orbitals $[3a_g1b_{3u}1b_{2u}1b_{2g}1b_{3g}3b_{1u}]$ within the framework of D_{2h} spatial symmetry.

Figure 2 displays the SSMRPT PECs for $X^3\Sigma_g^-$ O_2 obtained using the CASSCF and IVO-CASSCI orbitals. Figure 2

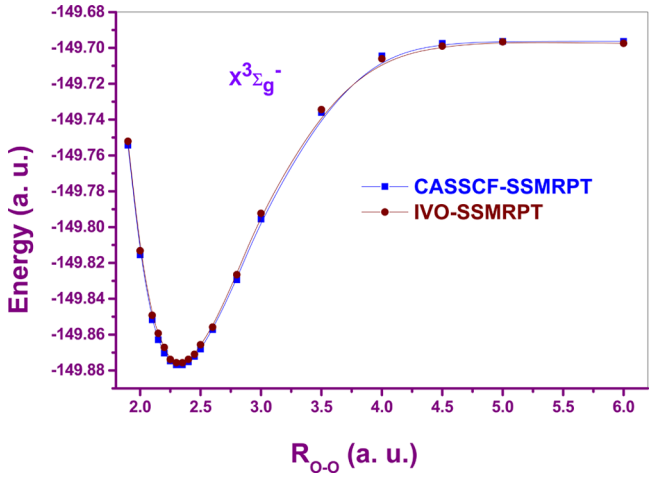

Figure 2. IVO-SSMRPT(8,6) and CASSCF-SSMRPT(8,6) energy curves for the dissociation of $^3\Sigma_g^-$ O_2 with the DZP basis set.

indicates that the SSMRPT approach with CASSCF and IVO-CASCI reference function allows a continuous transition from the strongly nondegenerate (single-reference) zone to the quasi-degenerate (MR) region without facing any difficulty of convergence. The IVO-SSMRPT and SSMRPT methods maintain acceptably small errors relative to FCI[135] [identified as $E_{FCI} - E_{Method}$] as assembled in Table 8. For a better understanding of the performance of the IVO-SSMRPT strategies, estimations of deviations/errors of the total electronic energy from the corresponding FCI value at a given interatomic distance R is more instructive in lieu of plotting the percentage of the correlation energy recovered. Such an analysis is more straightforward since the errors relative to the FCI values (ΔE) are independent of the definition of the uncorrelated reference wave function energy. It is observed that the deviation from the FCI values in case of the SSMRPT is small near the equilibrium geometry, and increases as one moves toward the dissociation regime. Enhancement of the errors of both SSMRPT methods in the dissociation region can be ascribed to the lack of higher-order correlation correction rather than to a failure of the approaches. In their MRCC calculations, Hubač, Pittner, and co-workers[138,139] have stated that the role of connected triples cannot be neglected in quantitative description of energy surface specially in the asymptotic limit. Note that the IVO-SSMRPT approach enjoys the advantage of demonstrating a more consistent behavior in terms of the relative errors from the FCI values. While the SSMRPT shows both positive and negative deviations with respect to the $X^3\Sigma_g^-$ FCI values, the IVO-SSMRPT, on the contrary, remains largely consistent throughout the PEC.

We have also extracted the spectroscopic parameters such as equilibrium bond distance, R_e, harmonic vibrational frequency, ω_e, and dissociation energy D_e. We have collected the extracted spectroscopic constants in Table 9. For comparison we have also tabulated CASPT2, MRMP2, and FCI values along with the experimental data (whenever available). Our extracted spectroscopic constants have also been compared with the other previously published values.[135−144] Tables 8 and 9 indicate that IVO-CASCI and CASSCF orbitals provide a good reference wave function for a perturbation calculation via

DOI: 10.1021/acs.jpca.6b03211
J. Phys. Chem. A 2016, 120, 5897−5916

Table 8. Errors (in millihartree) of the the Total Energies from FCI (au) for the $^3\Sigma_g^-$ State over Different Bond Lengths (au) in a DZP Basis Set[135,136] and a Theoretical Comparison between SSMRPT (with IVO-CASCI as Well as CASSCF Reference Function) and CASPT2

state	R	IVO-SSMRPT	CASSCF-SSMRPT	CASPT2D[a]	CASPT2N[a]	FCI
$^3\Sigma_g^-$	2.25	−1.334	−0.387	3.74	4.88	−149.875 15
	2.3	−1.294	−0.096	3.64	4.82	−149.876 95
	2.35	−1.019	0.188	3.55	4.76	−149.876 69
	2.40	−0.948	0.472			−149.874 74
	2.45	−0.469	0.704			−149.871 47
	100.0	−3.641	4.045	5.85	5.60	−149.706 68
$a^1\Delta_g$	2.25	−11.077	−11.831			−149.875 15
	2.3	−11.587	−11.617			−149.876 95
	2.35	−11.855	−11.759			−149.876 69
	2.40	−11.544	−11.71			−149.874 74
	2.45	−10.921	−11.66			−149.871 47
$b^1\Sigma_g^+$	2.25	−11.531	−11.835			−149.807 51
	2.3	−11.023	−11.672			−149.810 63
	2.35	−11.13	−11.848			−149.812 15
	2.40	−11.977	−11.848			−149.811 91
	2.45	−12.535	−11.846			−149.810 41

[a]Reference 136.

SSMRPT for $X^3\Sigma_g^-$ O_2. The differences between the CASSCF-SSMRPT and IVO-SSMRPT approaches are negligible. On comparison to FCI values, it is apparent that the performance of the IVO-SSMRPT method to yield spectroscopic constants is slightly better than that of the CASSCF-SSMRPT one. The SSMRPT results with CASSCF and IVO-CASCI orbitals for R_e, ω_e, and D_e are all in nice agreement with the results of CASPT2[136] and MRMP2. The implementation of SSMRPT method with IVO-CASCI reference function provided encouraging results that are in good agreement with benchmarks obtained by FCI.[135] A comparative study of the results of Hilbert space (HS) based MRCC approaches [such as Brillouin−Wigner (BW) and Mukherjee (Mk) formulation of MRCC schemes] by Pittner et al.[138,139] with our estimates allow an assessment of usefulness of the IVO-SSMRPT in comparison to the computationally demanding parent, full-blown MRCC methods. The spectroscopic constants due to IVO-SSMRPT calculations are in close agreement with MR-ccCA/cc-pVTZ values.[141] It is important to note that Bytautas and Ruedenberg[143] recently reported a value of 5.11 eV for the dissociation energy of O_2 obtained by the method of CEEIS/CBS scheme based on multiconfigurational RFORS(12,8)-reference function. Keeping in mind the perturbative nature, our IVO-SSMRPT result thereby also agrees well with the CEEIS one.

The results for the $a^1\Delta_g$ state are presented graphically in Figure 3. The PEC computed by the IVO-SSMRPT method is very smooth over the entire range of geometries indicating another useful measure for the effectiveness of our approach. The figure clearly illustrates that the shapes of PECs generated via CASSCF-SSMRPT and IVO-SSMRPT methods are very similar. The errors of the energies with respect to the FCI values in Table 8 amply in favor of the IVO-SSMRPT. The comparative analysis presented in Table 9 for the $a^1\Delta_g$ state indicates that the spectroscopic constants obtained with the IVO-SSMRPT are also in good accordance with the corresponding FCI values. It is also clear that our computed values are in well agreement with the results obtained by the computationally expensive calculations via HS-MRCC methods.[138,139] Thus, the quality of the excited $a^1\Delta_g$ state IVO-SSMRPT PEC is quite satisfactory in conjunction with a favorable trade-off between accuracy and computational cost.

First of all, as that of the other two states, it can be seen that the IVO-SSMRPT method yields smooth PEC of correct shape for the $b^1\Sigma_g^+$ state and is practically identical (see Figure 4). We observe that the topology of the IVO-SSMRPT and CASSCF-SSMRPT PECs are almost identical, which is also evident from the error values and extracted spectroscopic constants tabulated in Tables 8 and 9, respectively. Again, the errors, which are rather small, due to IVO-SSMRPT are seem to be very close to those of the SSMRPT. From Table 9, we may state that the spectroscopic parameters provided by the IVO-SSMRPT method are very close agreement with the corresponding FCI, and also with the available experimental results. Our IVO-SSMRPT results compare well with the HS-MRCC values. Here, we have also provided the excitation energies for $^3\Sigma_g^- \rightarrow a^1\Delta_g$ and $^3\Sigma_g^- \rightarrow b^1\Sigma_g^+$ which are 1.4001 and 2.011 eV, respectively, with the IVO-SSMRPT method, and 1.3439 and 2.087 eV, respectively, from the CASSCF-SSMRPT/DZP level of computations.[140] The corresponding transition energies for the FCI/DZP scheme are 1.082 and 1.823 eV respectively.[140] We have computed the excitation energies for each of the states that are involved using their respective equilibrium geometries. Therefore, there is a good overall agreement between the IVO-SSMRPT and SSMRPT transitions energies and they are also in close in proximity with the FCI values. The performance of the IVO-SSMRPT method is marginally better than the corresponding CASSCF-SSMRPT one. Here, we have also reported vertical transition (or excitation) energies (labeled as T_e) using the DZP basis at the experimental ground state geometry[145] in Table 10 along with the literature values for comparison. The result provided by our IVO-SSMRPT is close to that of the CASSCF-SSMRPT method. The agreements between IVO-SSMRPT theory and Mk- and BW version of MRCCSD(T) for vertical gap are fairly satisfactory for both the considered singlet states. The experimental values [0.982 eV for $a^1\Delta_g$ state and 1.636 eV for $b^1\Sigma_g^+$ state] given by Huber and Herzberg[145] are fairly compatible with our SSMRPT method with IVO-CASCI and CASSCF orbitals at DZP level. Note that the IVO-CASCI strategy combined with SSMRPT yield reliable

DOI: 10.1021/acs.jpca.6b03211
J. Phys. Chem. A 2016, 120, 5897−5916

Table 9. Spectroscopic Constants for the Ground and Excited States of O_2

state	reference	method	R_e (Å)	ω_e (cm^{-1})	D_e (eV)
$^3\Sigma_g^-$	present	IVO-SSMRPT/DZP	1.2310	1556	4.78
		CASSCF-SSMRPT/DZP	1.2316	1593	4.91
		MRMPPT/DZP	1.2298	1568	4.71
	136	CASPT2D/DZP	1.2280	1607	4.70
		CASPT2N/DZP	1.2260	1607	4.65
	135, 140	FCI/DZP	1.227	1642	4.64
	137	Werner CASPT2	1.2126	1566.1	5.12
		CASPT3	1.2076	1590.9	4.89
		Andersson CASMP2	1.2117	1585.4	5.31
		CASMP3	1.2063	1584.0	4.95
		Wolinski CASMP2	1.2116	1587.7	5.31
		CASMP3	1.2069	1579.6	4.93
		Dam CASMP2	1.2127	1587.2	5.33
		CASMP3	1.2070	1583.9	4.89
	138, 139	CCSD/cc-pVTZ	1.199	1679.1	
		CCSD(T)/cc-pVTZ	1.211	1589.6	
		4R-BWCCSD/cc-pVTZ	1.199	1683	
		4R-MkCCSD/cc-pVTZ	1.198	1686.6	
		4R-BWCCSD(T)/cc-pVTZ	1.2129	1577.4	
		4R-MkCCSD(T)/cc-pVTZ	1.2121	1582.1	
		8R-BWCCSD(T)/cc-pVTZ	1.2129	1576.7	
		8R-MkCCSD(T)/cc-pVTZ	1.2121	1582.1	
	141	icMRCI+Q/cc-pVTZ	1.2162	1557.6	
		MR-ccCA-P/cc-pVTZ	1.2069	1584.3	
	145	experiment	1.2075	1580	5.21
$a^1\Delta_g$	present work	IVO-SSMRPT/DZP	1.2334	1484.02	3.70
		CASSCF-SSMRPT/DZP	1.2387	1455.57	3.80
		MRMP2/DZP	1.2412	1463.6	3.68
	140	FCI/DZP	1.234	1539	3.61
	138, 139	4R-BWCCSD/cc-pVTZ	1.204	1628.4	
		4R-MkCCSD/cc-pVTZ	1.2049	1627.1	
		4R-BWCCSD(T)/cc-pVTZ	1.2193	1523.2	
		4R-MkCCSD(T)/cc-pVTZ	1.2147	1539.5	
		8R-BWCCSD(T)/cc-pVTZ	1.2165	1520.6	
		8R-MkCCSD(T)/cc-pVTZ	1.2161	1528.1	
	145	experiment	1.2155	1509.3	
$b^1\Sigma_g^+$	present work	IVO-SSMRPT/DZP	1.2525	1451.2	3.01
		CASSCF-SSMRPT/DZP	1.2528	1438.8	3.06
	140	FCI/DZP	1.2532	1517.0	2.87
	138, 139	4R-BWCCSD	1.211	1576.1	
		4R-MkCCSD/cc-pVTZ	1.2126	1570.3	
		4R-BWCCSD(T)/cc-pVTZ	1.2242	1472.7	
		4R-MkCCSD(T)/cc-pVTZ	1.2252	1465.6	
		8R-BWCCSD(T)/cc-pVTZ	1.2304	1426.8	
		8R-MkCCSD(T)/cc-pVTZ	1.2293	1437.6	
	145	experiment	1.2267	1432.6	

values for the vertical gaps of both the considered singlet states with a deviation from experiment of 0.084 and 0.167 eV for $a^1\Delta_g$ and $b^1\Sigma_g^+$ states, respectively. Vertical energy gap due to IVO-SSMRPT calculation compares fairly good with the DIP-based IH-FSMRCCSD results. The errors (eV) for the IH-FSMRCCSD level of calculation are 0.03 and 0.08 for $a^1\Delta_g$ and $b^1\Sigma_g^+$ states, respectively. The corresponding error for MRCISD with the Davidson correction (MRCISD+Q)and MRAQCC (MR average quadratic coupled cluster) are (0.025 and 0.059) and (0.019 and 0.02) respectively.[142] In the work of Müller,[142] we note that their computational approach encountered convergence problem owing to the state averaging procedure. Although application of the conventional FS-MRCC solutions are often plagued by intruder states, implementation of the intermediate Hamiltonian (IH) technique to the FS-MRCC method provides a robust approach for solving the FS-MRCC equations without facing convergence problems caused by these states and the presence of close-lying multiple solutions. As already mentioned, our IVO-SSMRPT method is free from any convergence problem due to intruder in a natural manner. The extensions of the dimension of the CAS in conjunction with the size of the basis set may lead to lowering the vertical energy gaps provide by our SSMRPT method. The above-mentioned quantitative surveys bolster our confidence about the applicability and usefulness of our IVO-SSMRPT scheme.

DOI: 10.1021/acs.jpca.6b03211
J. Phys. Chem. A 2016, 120, 5897−5916

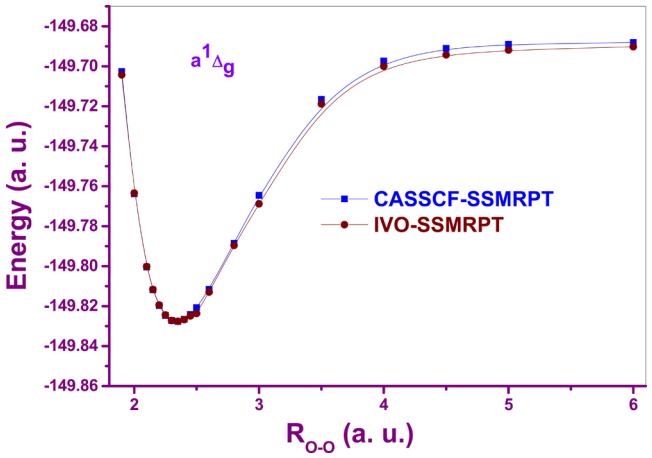

Figure 3. IVO-SSMRPT(8,6) and CASSCF-SSMRPT(8,6) energy curves for the dissociation of $a^1\Delta_g$ O_2 with the DZP basis set.

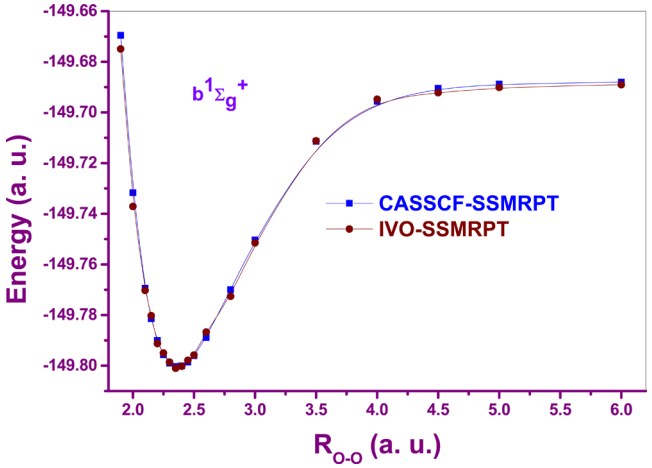

Figure 4. IVO-SSMRPT(8,6) and CASSCF-SSMRPT(8,6) energy curves for the dissociation of $b^1\Sigma_g^+$ O_2 with the DZP basis set.

Table 10. Comparison of Vertical Transition Energies (eV) for Two Lowest-Lying Singlet Excited States of O_2 with Respect to the Ground (Triplet) State: $T_e(1) = E_{^3\Sigma_g^-} \rightarrow E_{a^1\Delta_g}$ and $T_e(2) = E_{^3\Sigma_g^-} \rightarrow E_{b^1\Sigma_g^+}$

basis	method	$T_e(1)$	$T_e(2)$
present work	IVO-SSMRPT/DZP	1.110	1.851
	CASSCF-SSMRPT/DZP	1.127	1.843
138, 139	DIP-STEOM-CCSD/cc-pVTZ	1.066	1.803
	4R-BWCCSD/cc-pVTZ	1.058	1.902
	4R-MkCCSD/cc-pVTZ	0.995	1.790
	4R-BWCCSD(T)/cc-pVTZ	1.093	1.848
	4R-MkCCSD(T)/cc-pVTZ	1.030	1.736
	8R-BWCCSD(T)/cc-pVTZ	1.074	1.774
	8R-MkCCSD(T)/cc-pVTZ	1.016	1.671
144	IH-FS-CCSD(0,2)/cc-pCVQZ	1.011	1.718
142	MRCISD/cc-pVTZ	0.963	1.595
	MRCISD+Q/cc-pVTZ	1.007	1.695
	MRAQCC/cc-pVTZ	1.001	1.656
145	experimental	0.982	1.636

It has been experimentally established that the states $^3\Sigma_g^-$, $a^1\Delta_g$, and $b^1\Sigma_g^+$ tend to attain a near-/quasi-degenerate situation with an increasing O−O separation beyond the equilibrium internuclear positions. Figure 5 is a clear indication of the fact that these three states, when computed using the IVO-

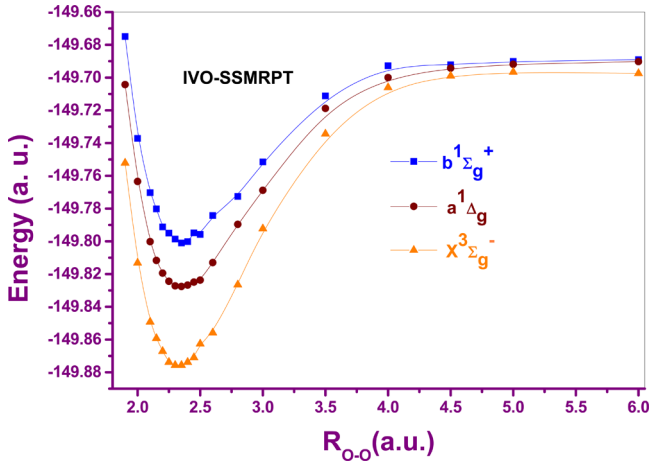

Figure 5. IVO-SSMRPT(8,6)/DZP dissociation energy curves for three lowest-lying states: $^3\Sigma_g^-$, $a^1\Delta_g$ and $b^1\Sigma_g^+$ of O_2 molecule.

SSMRPT, indeed maintain a quasi-degeneracy at the dissociation limit. From our present results we have found that the bond lengths become larger and the potential surfaces for the excited states becomes shallower compared to those for the ground state. The performance of SSMRPT method with IVO-CASCI and CASSCF orbitals for the excited states resembles that for the ground state. The present analysis indicate that our IVO-SSMRPT method allows one to break a double bond without involving further complications.

It should be noted that the PEC for $^3\Sigma_g^-$ O_2 can be estimated via standard single reference methods in principle. However, as noted in the literature,[144] the UHF-CCSD/cc-pCVTZ computations for $X^3\Sigma_g^-$ O_2 can be easily converged up to $2.5R_e$ [R_e stands for the equilibrium O−O bond distance equal to ca. 1.2 Å] and the performance of the UHF-CCSD(T)/cc-pCVTZ approach is fairly good in the equilibrium region, but goes down in the asymptotic region (i.e., for larger value of the range of interatomic O−O distances)exhibiting unwanted protuberance in the domain of $2R_e$. Olszówka and Musiał[144] found that CCSDT equations are converging only up to $1.5R_e$ for $X^3\Sigma_g^-$ O_2, beyond that region they do not converge at all. Olszówka and Musiał[144] demonstrated that the curves obtained from the different FSMRCC schemes behave differently. As for example, DIP-FSMRCCSD (IH-FSMRCC) curve shows a much consistent and better behavior as that of the DEA-based scheme over the wider range of O−O distances. Keeping in mind the topology of PECs depicted in Figures 1 and 2 in the published work of Olszówka and Musia,[144] we can say that our SSMRPT method mimics the overall shape of the computationally expensive curves provide by DIP strategy combined with the IH-FSMRCC approach over the entire range of inter nuclear distances (including the bond-breaking region) which is significantly beyond the limits of the other conventional effective Hamiltonian based MR based approaches. Moreover, although the methods considered here to gauge our results can be employed successfully to investigate various chemical properties and phenomena, they are also associated with few important objections, such as intruder states in the case of CASPT2, MRMPT2, or size-inextensivity in the case of BWMRCC, CASPT2, and MRMP2, or the restriction to states dominated by single excitations for EOM-based methods, and

DOI: 10.1021/acs.jpca.6b03211
J. Phys. Chem. A 2016, 120, 5897−5916

so on. Therefore, overall our IVO-SSMRPT values compare well with IH-FSMRCC and other HS-MRCC results. This fact indicates the clear benefit of using our SSMRPT approach. The most useful observation in the context of equilibrium geometrical parameters and other properties is that the IVO-SSMRT method is able to mimic the findings of the CCSD(T) [which has been often referred to as the "gold standard" of quantum chemistry], RMR-CCSD(T) and MRCC methods at a very low computational cost.

In totality, it is found that the values change marginally upon using IVO-CASCI orbitals instead of the naive CASSCF ones for all the three states considered here. We might enjoy the liberty to state that the IVO-SSMRPT is a strong contestant for the other MRPT strategies in vogue like the CASSCF-SSMRPT, CASPT2, MRMPPT, and so on, in addition to being one of the most useful approaches in terms of its ability to attribute the vital electronic correlation effects in a prudent manner in spite of its numerical simplicity. Thus, the IVO-SSMRPT gradient approach can be considered as a very effective and computationally viable model by means of which one can extend the range of application of the MR-based gradient method to large systems.

IV. CONCLUSION AND SUMMARIZING REMARKS

In the present paper, we have shown that one can develop a relatively inexpensive and easy-to-use *ab initio* method for high accuracy description of radicals such as methylene, benzyne, pyridyne, and pyridynium cation by combining the state-specific multireference second order perturbation theory (SSMRPT) method with an improved virtual orbital complete active space (CAS) configuration interaction (IVO-CASCI) along with the idea of using the multipartition MP scheme of H_0. Radicals have been the issue of various theoretical and experimental investigations overt the last few decades due to their high reactivity and significance as reactants, products, and intermediates in elementary chemical processes. A strong quasidegeneracy is inherent in such systems so that a MR treatment is more or less mandatory. The IVO-CASCI scheme circumvents iterations beyond the initial SCF approximation and CASSCF's attendant convergence difficulties. The resulting approach, denoted as IVO-SSMRPT, differs from popular MRPT methods (e.g., CASPT2, MRMP2, etc.) in the sense that the method is tailored to bypass intruders explicitly (so long as the target state energy remains well separated from the virtual functions) in a size-extensive manner. In IVO-SSMRPT method, the combining coefficients of the functions of the active space have been relaxed as a result of coupling of the nondynamical and dynamical correlations through the diagonalization of the effective Hamiltonian. The IVO-SSMRPT is based on the state universal ansatz of Jeziorski−Monkhorst (treats all reference functions democratically) and achieves state selectiveness by the exploiting suitable sufficiency condition. A IVO-SSMRPT wave function retains the attractive feature of the CASSCF-SSMRPT wave function. Numerical illustration shows that IVO-based scheme works quite well. We have also shown that the IVO-SSMRPT approach yields values which are in most cases comparable in accuracy with the CASSCF-SSMRPT calculations. The computed optimized geometrical parameters are comparable in accuracy with the best available *ab initio* methods such as Mk-MRCC, R-MRCC, etc., but at the same time they are significantly less demanding for computational resources, which indicates that the present approach can provide quantitative descriptions for all of the studied systems. The singlet−triplet gaps calculated by the present IVO-SSMRPT method are in close proximity with the available experimental values and other high level correlated *ab initio* estimates. For the ground state of O_2, the spectroscopic constants provided by IVO-SSMRPT are close to the results obtained from other established methods. Spectroscopic constants for the ground and excited states, and excitation energies for the lowest $a^1\Delta_g$, and $b^1\Sigma_g^+$ states are in fairly good agreements. The discussion on the performance of the IVO-SSMRPT *vis-á-vis* other established methods indicate that the IVO-SSMRPT method can provide correct description for multiple bond breaking processes.

All these merits (size-extensivity, intruder insensitivity, computational effectiveness, and IVO-CASCI framework) combined together, provide an excellent computational tool that is particularly effective for treating the ground and excited states of moderate-to-large MR systems (which deal with two types of electron correlation: nondynamic and dynamic) and is capable of providing good quality energy curves for the whole range of the internuclear distances with a favorable trade-off between accuracy and computational cost. We hope that the numerical values mentioned in this paper will motivate the MRPT method toward being more widely used, for instance in modeling of singlet−triplet gaps of various biradicals and chemical/biological process involving biradicaloid intermediates, like the ones encountered in the reactivity of the diradicaloids in DNA cleavage.

AUTHOR INFORMATION

Corresponding Author

*(S.C.) E-mail: sudip@chem.iiests.ac.in. Telephone: (91)(33) 26684561.

Notes

The authors declare no competing financial interest.

ACKNOWLEDGMENTS

Financial support from the DST, India, is gratefully acknowledged. S.S.R. thanks the UGC, India, for his research fellowship. A.G. acknowledges the DST, India, for an Inspire Fellowship.

REFERENCES

(1) Williams, W. P. E.; Jankiewicz, B. J.; Yang, L.; Kenttämaa, H. I. Properties and reactivity of gaseous distonic radical ions with aryl radical sites. *Chem. Rev.* **2013**, *113*, 6949−6985.

(2) Salem, L.; Rowland, C. The electronic properties of diradicals. *Angew. Chem., Int. Ed. Engl.* **1972**, *11*, 92−111.

(3) Borden, W. T. In *Diradicals*; Borden, W. T., Ed.; Wiley-Interscience: New York, 1982; p 1−72.

(4) Ramos-Cordoba, E.; Salvador, P. Characterization and quantification of polyradical character. *J. Chem. Theory Comput.* **2014**, *10*, 634−641.

(5) Nakajima, T.; Tsuneda, T.; Nakano, H.; Hirao, K. Recent advances in electronic structure theory. *J. Theor. Comput. Chem.* **2002**, *01*, 109−136.

(6) Roos, B. O.; Andersson, K.; Fülscher, M. P.; Malmqvist, P.-Å; Serrano-Andrés, L.; Pierloot, K.; Merchán, M. Multiconfigurational perturbation theory: Applications in electronic spectroscopy. *Adv. Chem. Phys.* **1996**, *93*, 219−331.

(7) Chaudhuri, R. K.; Freed, K. F.; Hose, G.; Piecuch, P.; Kowalski, K.; Włoch, M.; Chattopadhyay, S.; Mukherjee, D.; Rolik, Z.; Szabados, Á; Tóth, G.; Surjàn, P. R. Comparison of low-order multireference many-body perturbation theories. *J. Chem. Phys.* **2005**, *122*, 134105.

DOI: 10.1021/acs.jpca.6b03211
J. Phys. Chem. A 2016, 120, 5897−5916

(8) Hubać, I.; Wilson, S. *Progress in Theoretical Chemistry and Physics, Brillouin-Wigner methods for many-body systems*; Springer: New York, 2010; Vol. *21*.
(9) Chattopadhyay, S.; Chaudhuri, R. K.; Sinha Mahapatra, U.; Ghosh, A.; Sinha Ray, S. State-specific multireference perturbation theory: development and present status. *WIREs Comp. Mol. Sci.* **2016**, *6*, 266−291.
(10) Szalay, P. G.; Müller, T.; Gidofalvi, G.; Lischka, H.; Shepard, R. Multiconfiguration self-consistent field and multireference configuration interaction methods and applications. *Chem. Rev.* **2012**, *112*, 108−181. and references therein.
(11) *Recent Progress in Coupled Cluster Methods*; Čársky, P.; Paldus, J.; Pittner, J., Ed.; Springer: Dordrecht, The Netherlands, 2010; Vol. *11*.
(12) Kirtman, B. Simultaneous calculation of several interacting electronic states by generalized Van Vleck perturbation theory. *J. Chem. Phys.* **1981**, *75*, 798−808.
(13) Malrieu, J. P.; Durand, Ph.; Daudey, J. Intermediate Hamiltonians as a new class of effective Hamiltonians. *J. Phys. A: Math. Gen.* **1985**, *18*, 809−826.
(14) Andersson, K.; Malmqvist, P. A.; Roos, B. O.; Sadlej, A. J.; Wolinski, K. Second-order perturbation theory with a CASSCF reference function. *J. Phys. Chem.* **1990**, *94*, 5483−5488.
(15) Andersson, K.; Malmqvist, P. A.; Roos, B. O. Second-order perturbation theory with a complete active space self-consistent field reference function. *J. Chem. Phys.* **1992**, *96*, 1218−1226.
(16) Hirao, K. Multireference Møller-Plesset method. *Chem. Phys. Lett.* **1992**, *190*, 374−380.
(17) Hirao, K. Multireference MøllerPlesset perturbation treatment of potential energy curve ofN_2. *Int. J. Quantum Chem.* **1992**, *44* (S26), 517−526.
(18) Angeli, C.; Cimiraglia, R.; Evangelisti, S.; Leininger, T.; Malrieu, J.-P. Introduction of n-electron valence states for multireference perturbation theory. *J. Chem. Phys.* **2001**, *114*, 10252−10264.
(19) Angeli, C.; Bories, B.; Cavallini, A.; Cimiraglia, R. Third-order multireference perturbation theory: The n- electron valence state perturbation-theory approach. *J. Chem. Phys.* **2006**, *124*, 054108.
(20) Rintelman, J. M.; Adamovic, I.; Varganov, S.; Gordon, M. S. Multireference second-order perturbation theory: How size consistent is "almost size consistent. *J. Chem. Phys.* **2005**, *122*, 044105.
(21) Sen, A.; Sen, S.; Mukherjee, D. Aspects of size-consistency of Orbitally noninvariant size-extensive multireference perturbation theories: A case study using UGA-SSMRPT2 as a prototype. *J. Chem. Theory Comput.* **2015**, *11*, 4129−4145.
(22) Roos, B. O.; Andersson, K. Multiconfigurational perturbation theory with level shift - the Cr_2 potential revisited. *Chem. Phys. Lett.* **1995**, *245*, 215−223.
(23) Chang, S.-W.; Witek, H. A. Choice of optimal shift parameter for the intruder state removal techniques in multireference perturbation theory. *J. Chem. Theory Comput.* **2012**, *8*, 4053−4061. and reference therein.
(24) Choe, Y.-K.; Witek, H. A.; Finley, J. P.; Hirao, K. Identifying and removing intruder states in multireference Møller-Plesset perturbation theory. *J. Chem. Phys.* **2001**, *114*, 3913−3918.
(25) Camacho, C.; Witek, H. A.; Cimiraglia, R. The low-lying states of the scandium dimer. *J. Chem. Phys.* **2010**, *132*, 244306.
(26) Finley, J.; Malmqvist, P. Å; Roos, B. O.; Serrano-Andrés, L. The multi-state CASPT2 method. *Chem. Phys. Lett.* **1998**, *288*, 299−306.
(27) Nakano, H. Quasidegenerate perturbation theory with multiconfigurational self-consistent-field reference functions. *J. Chem. Phys.* **1993**, *99*, 7983−7992.
(28) Nakano, H.; Nakayama, K.; Hirao, K.; Dupuis, M. Transition state barrier height for the reaction $H_2CO \rightarrow H_2 + CO$ studied by multireference Møller-Plesset perturbation theory. *J. Chem. Phys.* **1997**, *106*, 4912−4917.
(29) Angeli, C.; Borini, S.; Cestari, M.; Cimiraglia, R. A quasidegenerate formulation of the second order n-electron valence state perturbation theory approach. *J. Chem. Phys.* **2004**, *121*, 4043−4049.
(30) Granovsky, A. A. Extended multi-configuration quasi-degenerate perturbation theory: The new approach to multi-state multi-reference perturbation theory. *J. Chem. Phys.* **2011**, *134*, 214113.
(31) Shiozaki, T.; Győrffy, W.; Celani, P.; Werner, H.-J. Communication: Extended multi-state complete active space second-order perturbation theory: Energy and nuclear gradients. *J. Chem. Phys.* **2011**, *135*, 081106.
(32) Sinha Mahapatra, U.; Datta, B.; Mukherjee, D. Molecular applications of a size-consistent state-specific multireference perturbation theory with relaxed model-space coefficients. *J. Phys. Chem. A* **1999**, *103*, 1822−1830.
(33) Evangelista, F. A.; Simmonett, A. C.; Schaefer, H. F., III; Mukherjee, D.; Allen, W. D. A companion perturbation theory for state-specific multireference coupled cluster methods. *Phys. Chem. Chem. Phys.* **2009**, *11*, 4728−4741.
(34) Sinha Mahapatra, U.; Chattopadhyay, S.; Chaudhuri, R. K. Molecular applications of state-specific multireference perturbation theory to HF, H_2O, H_2S, C_2, and N_2 molecules. *J. Chem. Phys.* **2008**, *129*, 024108.
(35) Sinha Mahapatra, U.; Chattopadhyay, S.; Chaudhuri, R. K. Application of state-specific multireference Møller-Plesset perturbation theory to nonsinglet states. *J. Chem. Phys.* **2009**, *130*, 014101.
(36) Sinha Mahapatra, U.; Chattopadhyay, S.; Chaudhuri, R. K. Second-order state-specific multireference Møller-Plesset perturbation theory (SS-MRMPPT) applied to geometry optimization. *J. Phys. Chem. A* **2010**, *114*, 3668−3682.
(37) Sinha Mahapatra, U.; Chattopadhyay, S.; Chaudhuri, R. K. Study of the ground state dissociation of diatomic molecular systems using state-specific multireference perturbation theory: A Brillouin-Wigner scheme. *J. Chem. Theory Comput.* **2010**, *6*, 662−682.
(38) Mao, S.; Cheng, L.; Liu, W.; Mukherjee, D. A spin-adapted size-extensive state-specific multi-reference perturbation theory. I. Formal developments. *J. Chem. Phys.* **2012**, *136*, 024105.
(39) Ghosh, A.; Chaudhuri, R. K.; Chattopadhyay, S.; Sinha Mahapatra, U. Relativistic state-specific multireference perturbation theory incorporating improved virtual orbitals: Application to the ground state single-bond dissociation. *J. Comput. Chem.* **2015**, *36*, 1954−1972.
(40) Schmidt, M. W.; Gordon, M. S. The construction and interpretation of MCSCF wavefunctions. *Annu. Rev. Phys. Chem.* **1998**, *49*, 233−266. and references therein.
(41) Potts, D. M.; Taylor, C. M.; Chaudhuri, R. K.; Freed, K. F. The improved virtual orbital-complete active space configuration interaction method, a "packageable" efficient ab initio many-body method for describing electronically excited states. *J. Chem. Phys.* **2001**, *114*, 2592−2600.
(42) Taylor, C. M.; Chaudhuri, R. K.; Freed, K. F. Electronic structure of the calcium monohydroxide radical. *J. Chem. Phys.* **2005**, *122*, 044317.
(43) Mazziotti, D. A. Contracted Schrödinger equation: Determining quantum energies and two-particle density matrices without wave functions. *Phys. Rev. A: At., Mol., Opt. Phys.* **1998**, *57*, 4219−4234.
(44) Kurashige, Y.; Chalupský, J.; Lan, T. N.; Yanai, T. Complete active space second-order perturbation theory with cumulant approximation for extended active-space wavefunction from density matrix renormalization group. *J. Chem. Phys.* **2014**, *141*, 174111.
(45) Sharma, S.; Chan, G. K.-L. Communication: A flexible multi-reference perturbation theory by minimizing the Hylleraas functional with matrix product states. *J. Chem. Phys.* **2014**, *141*, 111101.
(46) Chan, G. K.-L.; Head-Gordon, M. Highly correlated calculations with a polynomial cost algorithm: A study of the density matrix renormalization group. *J. Chem. Phys.* **2002**, *116*, 4462−4476.
(47) Hoffmann, M. R.; Helgaker, T. Use of density functional theory orbitals in the GVVPT2 variant of second-order multistate multi-reference perturbation theory. *J. Phys. Chem. A* **2015**, *119*, 1548−1553.
(48) Chattopadhyay, S.; Chaudhuri, R. K.; Sinha Mahapatra, U. Application of improved virtual orbital based multireference methods to N_2, LiF, and C_4H_6 systems. *J. Chem. Phys.* **2008**, *129*, 244108.

DOI: 10.1021/acs.jpca.6b03211
J. Phys. Chem. A 2016, 120, 5897−5916

(49) Chaudhuri, R. K.; Freed, K. F.; Chattopadhyay, S.; Sinha Mahapatra, U. Potential energy curve for isomerization of N_2H_2 and C_2H_4 using the improved virtual orbital multireference Møller-Plesset perturbation theory. *J. Chem. Phys.* **2008**, *128*, 144304.
(50) Chaudhuri, R. K.; Hammond, J. R.; Freed, K. F.; Chattopadhyay, S.; Sinha Mahapatra, U. Reappraisal of *cis* effect in 1,2-dihaloethenes: An improved virtual orbital multireference approach. *J. Chem. Phys.* **2008**, *129*, 064101.
(51) Chattopadhyay, S.; Chaudhuri, R. K.; Sinha Mahapatra, U. State-specific multireference perturbation theory with improved virtual orbitals: Taming the ground state of F_2, Be_2, and N_2. *J. Comput. Chem.* **2015**, *36*, 907−925.
(52) Chattopadhyay, S.; Chaudhuri, R. K.; Freed, K. F. Geometry optimization of radicaloid systems using improved virtual orbital-complete active space configuration interaction (IVO-CASCI) analytical gradient method. *J. Phys. Chem. A* **2011**, *115*, 3665−3678.
(53) Chattopadhyay, S.; Chaudhuri, R. K.; Sinha Mahapatra, U. Ab initio multireference investigation of disjoint diradicals: Singlet versus triplet ground states. *ChemPhysChem* **2011**, *12*, 2791−2797.
(54) Slipchenko, L. V.; Krylov, A. I. Singlet-triplet gaps in diradicals by the spin-flip approach: A benchmark study. *J. Chem. Phys.* **2002**, *117*, 4694−4708.
(55) Krylov, A. I.; Sherrill, C. D. Perturbative corrections to the equation-of-motion spin-flip self-consistent field model: Application to bond-breaking and equilibrium properties of diradicals. *J. Chem. Phys.* **2002**, *116*, 3194−3203.
(56) Krylov, A. I. Size-consistent wave functions for bond-breaking: The equation-of-motion spin-flip model. *Chem. Phys. Lett.* **2001**, *338*, 375−384.
(57) Hubač, I.; Mach, P.; Wilson, S. On the application of Brillouin-Wigner perturbation theory to multireference configuration mixing. *Mol. Phys.* **2002**, *100*, 859−863.
(58) Papp, P.; Mach, P.; Pittner, J.; Hubač, I.; Wilson, S. Many-body BrillouinWigner second-order perturbation theory using a multi-reference formulation: An application to bond breaking in the diatomic hydrides BH and FH. *Mol. Phys.* **2006**, *104*, 2367−2386.
(59) Rolik, Z.; Szabados, Å.; Surján, P. R. On the perturbation of multiconfiguration wave functions. *J. Chem. Phys.* **2003**, *119*, 1922−1928.
(60) Rosta, E.; Surján, P. R. Two-body zeroth order Hamiltonians in multireference perturbation theory: The APSG reference state. *J. Chem. Phys.* **2002**, *116*, 878−890.
(61) Jeszenszki, P.; Nagy, P. R.; Zoboki, T.; Szabados, Å.; Surján, P. R. Perspectives of APSG-based multireference perturbation theories. *Int. J. Quantum Chem.* **2014**, *114*, 1048−1052.
(62) Xu, E.; Li, S. Block correlated second order perturbation theory with a generalized valence bond reference function. *J. Chem. Phys.* **2013**, *139*, 174111.
(63) Liu, W.; Hoffmann, M. R. SDS: the 'static-dynamic-static' framework for strongly correlated electrons. *Theor. Chem. Acc.* **2014**, *133*, 1481.
(64) Malmqvist, P.-Å; Pierloot, K.; Shahi, A. R. M.; Cramer, C. J.; Gagliardi, L. The restricted active space followed by second-order perturbation theory method: Theory and application to the study of CuO_2 and Cu_2O_2 systems. *J. Chem. Phys.* **2008**, *128*, 204109.
(65) Nakano, H.; Nakatani, J.; Hirao, K. Second-order quasi-degenerate perturbation theory with quasi-complete active space self-consistent field reference functions. *J. Chem. Phys.* **2001**, *114*, 1133−1141.
(66) Nakano, H.; Uchiyama, R.; Hirao, K. Quasi-degenerate perturbation theory with general multiconfiguration self-consistent field reference functions. *J. Comput. Chem.* **2002**, *23*, 1166−1175.
(67) Staroverov, V. N.; Davidson, E. R. The reduced model space method in multireference second-order perturbation theory. *Chem. Phys. Lett.* **1998**, *296*, 435−444.
(68) Werner, H. Third-order multireference perturbation theory The CASPT3 method. *Mol. Phys.* **1996**, *89*, 645−661.
(69) Celani, P.; Werner, H.-J. Multireference perturbation theory for large restricted and selected active space reference wave functions. *J. Chem. Phys.* **2000**, *112*, 5546−5557.
(70) Hoffmann, M. R. Canonical Van Vleck quasidegenerate perturbation theory with trigonometric variables. *J. Phys. Chem.* **1996**, *100*, 6125−6130.
(71) Jiang, W.; Khait, Y. G.; Hoffmann, M. R. Configuration-driven unitary group approach for generalized Van Vleck variant multi-reference perturbation theory. *J. Phys. Chem. A* **2009**, *113*, 4374−4380.
(72) Barone, V.; Cacelli, I.; Ferretti, A.; Monti, S.; Prampolini, G. An integrated protocol for the accurate calculation of magnetic interactions in organic magnets. *J. Chem. Theory Comput.* **2011**, *7*, 699−706.
(73) Barone, V.; Boilleau, C.; Cacelli, I.; Ferretti, A.; Monti, S.; Prampolini, G. Structure-properties relationships in triplet ground state organic diradicals: A computational study. *J. Chem. Theory Comput.* **2013**, *9*, 300−307.
(74) Barone, V.; Boilleau, C.; Cacelli, I.; Ferretti, A.; Prampolini, G. Conformational effects on the magnetic properties of an organic diradical: A computational study. *J. Chem. Theory Comput.* **2013**, *9*, 1958−1963.
(75) Cacelli, I.; Ferretti, A.; Prampolini, G.; Barone, V. BALOO: A fast and versatile code for accurate multireference variational/perturbative calculations. *J. Chem. Theory Comput.* **2015**, *11*, 2024−2035.
(76) Jeziorski, B.; Monkhorst, H. J. Coupled-cluster method for multideterminantal reference states. *Phys. Rev. A: At., Mol., Opt. Phys.* **1981**, *24*, 1668−1681.
(77) Taube, A. G.; Bartlett, R. J. Rethinking linearized coupled-cluster theory. *J. Chem. Phys.* **2009**, *130*, 144112.
(78) Szabados, Å. Sensitivity analysis of state-specific multireference perturbation theory. *J. Chem. Phys.* **2011**, *134*, 174113.
(79) Zaitsevskii, A.; Malrieu, J. P. Multi-partitioning quasidegenerate perturbation theory. A new approach to multireference Møller-Plesset perturbation theory. *Chem. Phys. Lett.* **1995**, *233*, 597−604.
(80) McWilliams, D.; Huzinaga, S. Nature of virtual orbitals in minimum-basis set calculations. *J. Chem. Phys.* **1971**, *55*, 2604−2605.
(81) Martin, J. M. L. Spectroscopic quality ab initio potential curves for CH, NH, OH and HF. A convergence study. *Chem. Phys. Lett.* **1998**, *292*, 411−420.
(82) Bauschlicher, C. W.; Taylor, P. R. A full CI treatment of the $^1A_1$-$^3B_1$ separation in methylene. *J. Chem. Phys.* **1986**, *85*, 6510−6512.
(83) Bauschlicher, C. W., Jr. Is the $\tilde{c}$ state of CH_2 linear or bent? *Theor. Chem. Acc.* **1997**, *96*, 11−13.
(84) Yamaguchi, Y.; Sherrill, C. D.; Schaefer, H. F., III The $\tilde{X}^3B_1$, $\tilde{a}^1A_1$, $\tilde{b}^1B_1$, and $\tilde{c}^1A_1$ Electronic States of CH_2. *J. Phys. Chem.* **1996**, *100*, 7911−7918.
(85) Sherrill, C. D.; Leininger, M. L.; Van Huis, T. J.; Schaefer, H. F., III Structures and vibrational frequencies in the full configuration interaction limit: Predictions for four electronic states of methylene using a triple-zeta plus double polarization (TZ2P) basis. *J. Chem. Phys.* **1998**, *108*, 1040−1049.
(86) Li, X.; Paldus, J. Simultaneous handling of dynamical and nondynamical correlation via reduced multireference coupled cluster method: Geometry and harmonic force field of ozone. *J. Chem. Phys.* **1999**, *110*, 2844−2852.
(87) Li, X.; Paldus, J. Electronic structure of organic diradicals: Evaluation of the performance of coupled-cluster methods. *J. Chem. Phys.* **2008**, *129*, 174101.
(88) Shiozaki, T.; Werner, H.-J. Communication: Second-order multireference perturbation theory with explicit correlation: CASPT2-F12. *J. Chem. Phys.* **2010**, *133*, 141103.
(89) Włoch, M.; Gour, J. R.; Piecuch, P. Extension of the renormalized coupled-cluster methods exploiting left eigenstates of the similarity-transformed Hamiltonian to open-shell systems: A benchmark study. *J. Phys. Chem. A* **2007**, *111*, 11359−11382.
(90) Shen, J.; Piecuch, P. Merging active-space and renormalized coupled-cluster methods via the CC (P; Q) formalism, with

DOI: 10.1021/acs.jpca.6b03211
J. Phys. Chem. A 2016, 120, 5897−5916

benchmark calculations for singlet-triplet gaps in biradical systems. *J. Chem. Theory Comput.* **2012**, *8*, 4968−4988.
(91) Shen, J.; Fang, T.; Hua, W.; Li, S. Spectroscopic constants of single-bond diatomic molecules and singlet-triplet gaps of diradicals by the block-correlated coupled cluster theory. *J. Phys. Chem. A* **2008**, *112*, 4703−4709.
(92) Feller, D.; Peterson, K.; Hill, J. G. Calibration study of the CCSD (T)-F12a/b methods for C_2 and small hydrocarbons. *J. Chem. Phys.* **2010**, *133*, 184102.
(93) Liu, W.; Hoffmann, M. R. SDS: the 'static-dynamic-static'framework for strongly correlated electrons. *Theor. Chem. Acc.* **2014**, *133*, 1481.
(94) Kerkines, I. S. K.; Čársky, P.; Mavridis, A. A multireference coupled-cluster potential energy surface of diazomethane, CH_2N_2. *J. Phys. Chem. A* **2005**, *109*, 10148−10152.
(95) Liu, X.; Bian, W.; Zhao, X.; Tao, X. Potential energy surface intersections in the C (^1D) H_2 reactive system. *J. Chem. Phys.* **2006**, *125*, 074306.
(96) See www.emsl.pnl.gov/forms/basisform.html. Schuchardt, K. L.; Didier, B. T.; Elsethagen, T.; Sun, L.; Gurumoorthi, V.; Chase, J.; Li, J.; Windus, T. L. Basis Set Exchange: A Community Database for Computational Sciences. *J. Chem. Inf. Model.* **2007**, *47*, 1045−1052. and references therein.
(97) Pittner, J.; Šmydke, J. Analytic gradient for the multireference Brillouin-Wigner coupled cluster method and for the state-universal multireference coupled cluster method. *J. Chem. Phys.* **2007**, *127*, 114103.
(98) Demel, O.; Pittner, J. Multireference Brillouin-Wigner coupled cluster method with singles, doubles, and triples: Efficient implementation and comparison with approximate approaches. *J. Chem. Phys.* **2008**, *128*, 104108.
(99) Petek, H.; Nesbitt, D. J.; Darwin, D. C.; Ogilby, P. R.; Moore, C. B.; Ramsay, D. A. Analysis of $CH_2\tilde{a}^1A_1$ (1, 0, 0) and (0, 0, 1) Coriolis-coupled states, $\tilde{a}^1A_1$ - $\tilde{X}^3B_1$ spin-orbit coupling, and the equilibrium structure of CH_2 $\tilde{a}^1A_1$ state. *J. Chem. Phys.* **1989**, *91*, 6566−6578.
(100) Flores, J. R.; Gdanitz, R. J. Accurately solving the electronic Schrodinger equation of small atoms and molecules using explicitly correlated (r12-) MR-CI. VIII. Valence excited states of methylene (CH_2). *J. Chem. Phys.* **2005**, *123*, 144316.
(101) Zen, A.; Coccia, E.; Luo, Y.; Sorella, S.; Guidoni, L. Static and dynamical correlation in diradical molecules by quantum Monte Carlo using the Jastrow antisymmetrized geminal power ansatz. *J. Chem. Theory Comput.* **2014**, *10*, 1048−1061.
(102) Jensen, P.; Bunker, P. R. The potential surface and stretching frequencies of $\tilde{X}^3B_1$ methylene (CH_2) determined from experiment using the Morse oscillator-rigid bender internal dynamics Hamiltonian. *J. Chem. Phys.* **1988**, *89*, 1327−1332.
(103) Perera, A.; Molt, R. W., Jr.; Lotrich, V. F.; Bartlett, R. J. Singlet-triplet separations of di-radicals treated by the DEA/DIP-EOM-CCSD methods. *Theor. Chem. Acc.* **2014**, *133*, 1514.
(104) Jagau, T.-C.; Gauss, J. Ground and excited state geometries via Mukherjee's multireference coupled-cluster method. *Chem. Phys.* **2012**, *401*, 73−87.
(105) Jagau, T.-C.; Prochnow, E.; Evangelista, F. A.; Gauss, J. Analytic gradients for Mukherjee's multireference coupled-cluster method using two-configurational self-consistent-field orbitals. *J. Chem. Phys.* **2010**, *132*, 144110.
(106) Woon, D. E.; Dunning, T. H., Jr. Gaussian basis sets for use in correlated molecular calculations. V. Core-valence basis sets for boron through neon. *J. Chem. Phys.* **1995**, *103*, 4572−4585.
(107) Prochnow, E.; Evangelista, F. A.; Schaefer, H. F., III; Allen, W. D.; Gauss, J. Analytic gradients for the state-specific multireference coupled cluster singles and doubles model. *J. Chem. Phys.* **2009**, *131*, 064109.
(108) Evangelista, F. A.; Prochnow, E.; Gauss, J.; Schaefer, H. F., III Perturbative triples corrections in state-specific multireference coupled cluster theory. *J. Chem. Phys.* **2010**, *132*, 074107.
(109) Wenthold, P. G.; Squires, R. R.; Lineberger, W. C. Ultraviolet Photoelectron Spectroscopy of the o-, m-, and p-Benzyne Negative Ions. Electron Affinities and Singlet-Triplet Splittings for o-, m-, and p-Benzyne. *J. Am. Chem. Soc.* **1998**, *120*, 5279−5290.
(110) Marquardt, R.; Sander, W.; Kraka, E. 1, 3-Didehydrobenzene (m-Benzyne). *Angew. Chem., Int. Ed. Engl.* **1996**, *35*, 746−748.
(111) Sander, W. m-Benzyne. and p-Benzyne. *Acc. Chem. Res.* **1999**, *32*, 669−676.
(112) Sander, W.; Exner, M.; Winkler, M.; Balster, A.; Hjerpe, A.; Kraka, E.; Cremer, D. Vibrational spectrum of m-benzyne: A matrix isolation and computational study. *J. Am. Chem. Soc.* **2002**, *124*, 13072−13079.
(113) Cramer, C. J.; Nash, J. J.; Squires, R. R. A reinvestigation of singlet benzyne thermochemistry predicted by CASPT2, coupled-cluster and density functional calculations. *Chem. Phys. Lett.* **1997**, *277*, 311−320.
(114) Kraka, E.; Cremer, D. Ortho-, meta-, and para-benzyne. A comparative CCSD(T) investigation. *Chem. Phys. Lett.* **1993**, *216*, 333−340.
(115) Kraka, E.; Anglada, J.; Hjerpe, A.; Filatov, M.; Cremer, D. m-Benzyne and bicyclo [3.1.0] hexatriene-which isomer is more stable?-a quantum chemical investigation. *Chem. Phys. Lett.* **2001**, *348*, 115−125.
(116) de Visser, S. P.; Filatov, M.; Shaik, S. REKS calculations on ortho-, meta-and para-benzyne. *Phys. Chem. Chem. Phys.* **2000**, *2*, 5046−5048.
(117) Kraka, E.; Anglada, J.; Hjerpe, A.; Filatov, M.; Cremer, D. m-Benzyne and bicyclo [3.1.0] hexatriene-which isomer is more stable?-a quantum chemical investigation. *Chem. Phys. Lett.* **2001**, *348*, 115−125.
(118) Winkler, M.; Sander, W. The Structure of meta-benzyne revisited a close look into σ-bond formation. *J. Phys. Chem. A* **2001**, *105*, 10422−10432.
(119) Leung, J. W.-H.; Wang, X.; Cheung, A. S.-C. Laser spectroscopy of NiBr: Ground and low-lying electronic states. *J. Chem. Phys.* **2002**, *117*, 3694−3700.
(120) Manohar, P. U.; Krylov, A. I. A noniterative perturbative triples correction for the spin-flipping and spin-conserving equation-of-motion coupled-cluster methods with single and double substitutions. *J. Chem. Phys.* **2008**, *129*, 194105.
(121) Smith, C. E.; Crawford, T. D.; Cremer, D. The structures of m-benzyne and tetrafluoro-m-benzyne. *J. Chem. Phys.* **2005**, *122*, 174309. and references therein.
(122) Li, H.; Yu, S.-Y.; Huang, M.-B.; Wang, Z.-X. The S1 states of o-, m-, and p-benzyne studied using multiconfiguration second-order perturbation theory. *Chem. Phys. Lett.* **2007**, *450*, 12−18.
(123) Al-Saidi, W. A.; Umrigar, C. J. Fixed-node diffusion Monte Carlo study of the structures of m-benzyne. *J. Chem. Phys.* **2008**, *128*, 154324.
(124) Chattopadhyay, S.; Chaudhuri, R. K.; Sinha Mahapatra, U. Studies on m-benzyne and phenol via improved virtual orbital-complete active space configuration interaction (IVO-CASCI) analytical gradient method. *Chem. Phys. Lett.* **2010**, *491*, 102−108.
(125) Hess, J. Do Bicyclic Forms of m-and p-benzyne Exist? *Eur. J. Org. Chem.* **2001**, *2001* (11), 2185−2189.
(126) Kraka, E.; Cremer, D.; Bucher, G.; Wandel, H.; Sander, W. A CCSD(T) and DFT investigation of m-benzyne and 4-hydroxy-m-benzyne. *Chem. Phys. Lett.* **1997**, *268*, 313−320.
(127) Debbert, S. L.; Cramer, C. J. Systematic comparison of the benzynes, pyridynes, and pyridynium cations and characterization of the Bergman cyclization of Z-but-1-en-3-yn-1-yl isonitrile to the meta diradical 2,4-pyridyne. *Int. J. Mass Spectrom.* **2000**, *201*, 1−15.
(128) Wenk, H. H.; Sander, W. Generation of fluorinated m-Benzyne derivatives in neon matrices. *Eur. J. Org. Chem.* **2002**, *2002* (23), 3927−3935.
(129) Thoen, K. K.; Kenttämaa, H. I. Reactivity of a substituted m-benzyne biradical. *J. Am. Chem. Soc.* **1999**, *121*, 800−805.
(130) Evangelista, F. A.; Allen, W. D.; Schaefer, H. F., III Coupling term derivation and general implementation of state-specific multi-reference coupled cluster theories. *J. Chem. Phys.* **2007**, *127*, 024102.

DOI: 10.1021/acs.jpca.6b03211
J. Phys. Chem. A 2016, 120, 5897−5916

(131) Hanauer, M.; Köhn, A. Pilot applications of internally contracted multireference coupled cluster theory, and how to choose the cluster operator properly. *J. Chem. Phys.* **2011**, *134*, 204111.
(132) Rinkevicius, Z.; Ågren, H. Spin-flip time dependent density functional theory for singlet-triplet splittings in σ, σ -biradicals. *Chem. Phys. Lett.* **2010**, *491*, 132−135.
(133) Schreiner, P. R.; Prall, M.; Lutz, V. Fulvenes from enediynes: Regioselective electrophilic domino and tandem cyclizations of enynes and oligoynes. *Angew. Chem., Int. Ed.* **2003**, *42*, 5757−5760.
(134) Li, X.; Paldus, J. Reduced multireference coupled-cluster method and its application to the pyridyne diradicals. *J. Theor. Comput. Chem.* **2008**, *07*, 805−820.
(135) Bauschlicher, C. W.; Langhoff, S. R. Full CI benchmark calculations on N_2, NO, and O_2: A comparison of methods for describing multiple bonds. *J. Chem. Phys.* **1987**, *86*, 5595−5599.
(136) Andersson, K.; Malmqvist, P. Å; Roos, B. O. Second-order perturbation theory with a complete active space self-consistent field reference function. *J. Chem. Phys.* **1992**, *96*, 1218−1226.
(137) Van Dam, H. J. J.; Van Lenthe, J. H.; Pulay, P. The size consistency of multi-reference Møller-Plesset perturbation theory. *Mol. Phys.* **1998**, *93*, 431−439.
(138) Pittner, J.; Čársky, P.; Hubač, I. Four-and 8-reference state-specific Brillouin-Wigner coupled-cluster method: Study of the singlet oxygen. *Int. J. Quantum Chem.* **2002**, *90*, 1031−1037.
(139) Bhaskaran-Nair, K.; Demel, O.; Pittner, J. Multireference state-specific Mukherjee's coupled cluster method with noniterative triexcitations. *J. Chem. Phys.* **2008**, *129*, 184105.
(140) Chattopadhyay, S.; Sinha Mahapatra, U.; Chaudhuri, R. K. Investigation of low-lying states of oxygen molecule via second-order multireference perturbation theory: A state-specific approach. *J. Phys. Chem. A* **2009**, *113*, 5972−5984.
(141) Jiang, W.; Wilson, A. K. Multireference composite approaches for the accurate study of ground and excited electronic states: C_2, N_2, and O_2. *J. Chem. Phys.* **2011**, *134*, 034101.
(142) Müller, T.; Dallos, M.; Lischka, H.; Dubrovay, Z.; Szalay, P. G. A systematic theoretical investigation of the valence excited states of the diatomic molecules B_2, C_2, N_2 and O_2. *Theor. Chem. Acc.* **2001**, *105*, 227−243.
(143) Bytautas, L.; Ruedenberg, K. Accurate ab initio potential energy curve of O_2 I. Nonrelativistic full configuration interaction valence correlation by the correlation energy extrapolation by intrinsic scaling method. *J. Chem. Phys.* **2010**, *132*, 074109.
(144) Olszówka, M.; Musiał, M. Coupled cluster calculations in the (0,2) and (2,0) sectors of the Fock space for the lowest electronic states of the O_2 molecule. *Mol. Phys.* **2014**, *112*, 609−615.
(145) Huber, K. P.; Herzberg, G. *Molecular spectra and molecular structure, IV. constants of diatomic molecules*; Von Nostrand: New York, 1979.

DOI: 10.1021/acs.jpca.6b03211
J. Phys. Chem. A 2016, 120, 5897−5916